JPRS-UPM-90-005
28 NOVEMBER 1990

JPRS Report

Science & Technology

USSR: Physics & Mathematics

Science & Technology
USSR: Physics & Mathematics

JPRS-UPM-90-005 *28 November 1990*

CONTENTS

Lasers

Nuclear Physics

Optics, Spectroscopy

Plasma Physics

Superconductivity

Theoretical Physics

Numerical Analysis, Algorithms

Probability, Statistics

Evolution of Vibrational Molecule Distribution Function and of Flow Pattern in Relaxation Zone behind Front of Standing Shock Wave in Vibrationally Excited Molecular Gas

907J0028D Leningrad ZHURNAL TEKHNICHESKOY FIZIKI in Russian Vol 60 No 2, Feb 90 pp 22-31

[Article by K.G. Gureyev and V.O. Zolotarev]

[Abstract] Gasdynamic flow behind the front of a standing shock wave in a vibrationally excited molecular gas is analyzed on the basis of a simplified model, this model describing a gas at such a degree of nonequilibrium and a shock wave of such intensity that excitation of electronic levels and the effect of dissociation are negligible. The properties of the gas immediately behind the shock-wave front (x = 0) are defined by a system of three Hugoniot relations and normalized to the initial conditions including the speed of sound immediately before the shock-wave front. Evolution of the distribution of molecules over vibrational levels behind the shock-wave front is described by a system of three equations and the equation of state, disregarding viscosity as well as heat transfer by conduction and radiation. Only single transitions of molecules are considered in the description of vibrational exchange processes according to the Morse model of anharmonic oscillators and in the expressions for VT and VV exchange constants according to the SSH-theory. Evolution of the gas flow pattern in the relaxation zone behind the shock-wave front is described by a system of four equations, the model for this description having been simplified by assuming a quasi-steady distribution of molecules over vibrational levels. Simultaneous numerical integration of all differential equation has yielded the dependence of the characteristic relaxation time for vibrational energy of nitrogen molecules on the average energy of their vibrational excitation at various gas temperatures, the dependence of the T_V(K)-p_0x(Pa.cm) profile and the density profile ρ/ρ_0-p_0x(Pa.cm) ((T_V-vibrational temperature, ρ_0- initial density of gas, p_0- initial pressure, x-distance from shock-wave front) on the initial gas nonequilibrium index and on the initial gas temperature. These profiles indicate a fast restructurization of the distribution of gas molecules over vibrational levels behind the shock-wave front, a complete population inversion in vibrational levels taking place in the case of high initial gas nonequilibrium index. They also indicate a nonmonotonic T_{V1} distribution (T_{V1} - temperature of first vibrational level) along the relaxation zone behind the shock-wave front and a nonmonotonic distribution of the gas temperature behind the shock-wave front with a steep rise followed by very slight droop in the case of a high initial gas nonequilibrium index. The error of calculations on the basis of this model is large at small distances behind the shock-wave front, but the estimated width of the relaxation zone is off by not more than 30% and adequately accurate for rough analysis, not concerned about the fine structure of this layer. The authors thank V.V. Anfinogenov for helpful discussions. Figures 7; references 24.

UDC 534.286.2

Absorption of Sound in Melts of Gallium and Indium Tellurides

907J0043A Moscow TEPLOFIZIKA VYSOKIKH TEMPERATUR in Russian Vol 28 No 1, Jan-Feb 90 pp 69-74

[Article by V.M. Glazov, S.G. Kim, and T. Suleymenov, Moscow Institute of Electronics Engineering]

[Abstract] A method of measuring the acoustic absorption coefficient has been developed especially for a determination of its temperature dependence in melts of GaTe, Ga_2Te_3 and InTe, In_2Te_3 produced from Ga-000 gallium, In-00 indium, and TA-1 tellurium, these tellurides being known to retain their semiconductor characteristics at temperatures above the melting point. The method involves use of a high-voltage sine-wave oscillator and a generator of square pulses of 1-5 μs duration. These pulses, generated at a repetition rate of 2 kHz, modulate the sinusoidal voltage into radio pulses which, after passage through a matching waveguide, provide the necessary excitation for a piezoelectric radiator-transducer in the for of an X-cut quartz disk with a 10 MHz fundamental resonance frequency. Ultrasonic pulses generated by this radiator pass through a stationary lower sound guide and then through the melt, from where they are passed through a movable upper sound guide and are then picked up by a piezoelectric receiver-transducer which generates electric radio pulses transmitted to a superheterodyne radio receiver. The performance of the piezoelectric transducer pair is monitored by and compared with that of a reference cell consisting of a similar transducer pair and a similar sound guide, in effect also serving as an acoustic delay line. While measurements in the test cell cover a wide temperature range, the reference cell remains under thermostatic control. The advantages of this method over standard include low sensitivity to angular and axial displacement of the sound guide and short stabilization time at a new temperature. Measurements by this method were made with the melt sounded by signals at frequencies corresponding to odd harmonics of quartz disk vibration, from the third (30 MHz) to the thirteenth (130 MHz), once with the upper sound guide fixed in its lower position and once with the lower sound guide fixed in an upper position so that correspondingly two sets of absorption (signal amplitude) isotherms were thus obtained. Measurements were first made with an indium melt, over the 435-770 K temperature range and then with melts of the four tellurides in the test cell: In_2Te_3 (965-1095 K), InTe (980-1097 K), Ga_2Te_3 (1065-1220 K), GaTe (1100-1228 K). The results of these measurements, indicating a decrease of the absorption coefficient normalized to the frequency squared with rising temperature, are compared with available experimental data on the temperature dependence of the speed of sound in these melts. In the melts of gallium tellurides the absorption coefficient and the speed of sound are found to change symbiotically throughout the entire temperature

range. In the melt of InTe they are found to change adiabatically throughout the entire temperature range. In the In_2Te_3 melt they are found to change symbiotically up to about 1025 K and adiabatically above 1025 K, the speed of sound being minimum at that temperature evidently corresponding to a change the thermal breakdown mechanism. Figures 6; tables 1; references 8.

UDC 533.697.4

Vibratory Nonequilibrium Flow of CO + Ar Gas Mixture Through Profiled Supersonic Nozzle

907J0043B Moscow TEPLOFIZIKA VYSOKIKH TEMPERATUR in Russian Vol 28 No 1, Jan-Feb 90 pp 75-81

[Article by V.V. Kalyuzhnyy and V.V. Kotelnikov, Moscow]

[Abstract] Vibratory nonequilibrium flow of a CO + Ar mixture through a nozzle is analyzed, assuming this gas to be an ideal and nonviscous one which does not conduct heat. Three kinds of one-quantum processes are included, namely spontaneous emission of radiation during transition of a CO molecule from level v to level v-1 as well as reversible processes of vibrational-translational and vibrational-vibrational relaxation during transitions of a CO molecule from level v to level v-1 or of two CO molecules from level v to level v-1 and from level w to level w+1 respectively (v,w = 1,..., V_{max} = 20). Existence of a boundary layer is taken into account by correction of the nozzle profile for the displacement thickness. Assuming a negligible effect of vibrational relaxation of CO molecules on the gasdynamic parameters, the analysis is simplified by first calculating the flow parameters, namely pressure and velocity, along streamlines and then, with the aid of the thus obtained pressure distributions, solving the conventional one-dimensional equations of mass-energy-momentum conservation as well as the equation of kinetics for the rate of change of concentration at vibrational levels of CO. Two sets of calculations have been made for a one-dimensional supersonic flow of two different mixtures with a nominal Mach number N_{Ma} = 5 at the edge of an axisymmetric nozzle with a camber. The two mixtures contained 0.093 and 0.101 molar fractions of CO respectively. The stagnation temperature and pressure were 2400 K and 0.704 in the first case, 2000 K and 0.667 MPa in the second case. The theoretical data agree satisfactorily with available experimental data pertaining to these two mixtures, the differences not being larger than the measurement error. The data cover distribution of CO molecules over vibrational levels, dependence of the weak-signal gain at the vibrational-rotational $P_7(3)$ transition on the stagnation temperature and pressure, and distribution along streamlines of the weak-signal gain at the $P_7(3)$ transitions. Calculations have therefore been extended to a mixture containing a 0.3 molar fraction of CO and flowing with Mach numbers N_{Ma} = 8 and 11, with a 2500 K stagnation temperature 2500 K and a 10 MPa stagnation pressure. The data on flow of this mixture include distributions along streamlines of the weak-signal gain at both $P_7(12)$ and P_612 transitions. The authors thank N.B. Ponomarev for assisting in calculation of the gasdynamic parameters. Figures 5; references 30.

UDC 536.75:533.72

Equations of Transfer and Approximate Equation of Kinetics for Moderately Dense Gas of Molecules With Solid Core

907J0043C Moscow TEPLOFIZIKA VYSOKIKH TEMPERATUR in Russian Vol 28 No 1, Jan-Feb 90 pp 40-46

[Article by V.I. Kurochkin, Institute of Physics imeni P.N. Lebedev, USSR Academy of Sciences]

[Abstract] On the basis of the system of BBGKI (Boltzmann-Bogolyubov-Gordon-Klein-Ito) equations describing the dynamics of s-particle distribution functions, an approximate extension of the Enskog equation of kinetics is obtained for a gas of molecules consisting of solid spheres separated by distances larger than their diameters so that their interaction potential equals the potential of spheres plus a much smaller than kT "tail" potential of long-distance interaction. Equations of energy and momentum transfer are then derived for calculation of mass density, hydrodynamic velocity, and internal energy, whereupon the solution to the new equation of kinetics is sought in the form of series with respect to the gas nonhomogeneity parameter. An expression for the equilibrium pressure is obtained from that solution in the zeroth approximation. This expression is found to be the same as the one according to the equilibrium statistical theory. References 8.

UDC 539.4+548.4

Sequence of Events in Strain Structure Development in Al and Cu Single Crystals Under Shock Loads of up to 50 GPa and 100 GPa Respectively

907J0046A Novosibirsk FIZIKA GORENIYA I VZRYVA in Russian Vol 26 No 2, Mar-Apr 90 pp 95-102

[Article by M.A. Mogilevskiy and L.S. Bushnev, Novosibirsk]

[Abstract] An experimental study of structural changes produced in single crystals of aluminum and copper by shock waves of 20-50 GPa and 5-100 GPa respectively. Single crystals 20 mm long and 15 mm square in cross-section, those of copper with [110],[112] orientations and those of aluminum with [110],[113] orientations, were held in a conical clamp and struck by 2 mm thick plates of stainless steel plates driven by shock at

velocities necessary for generating the necessary pressure. Such shock waves were in turn generated by explosion of charge. The residual strains were 0.01 in copper crystals after impact by a 100 GPa shock wave and 0.06 in aluminum crystals after impact by a 50 GPa shock wave. After impact by shock waves of successively higher pressures, the crystals were dropped into water for subsequently microstructural examination under an optical microscope and measurements in an electron diffractometer. An analysis of the thus obtained pressure dependence of the strain structure does not support Cowan's theory of a "supercritical shearing stress" under intermediate shock pressures and indicates a much higher shearing stress necessary for loss of lattice stability. The data reveal a slow-down and eventual suppression of the twinning process in Cu single crystals, dislocations evidently moving and stresses correspondingly relaxing much faster under high-pressure impact. Plastic deformation under impact is best explained by heterogeneous origins of dislocations and by high concentration of point defects. The extremely small distances between dislocations being, other than high temperatures, a principal factor contributing not only to realignment of strains during the final compression stage and then during holding under the maximum pressure but also during subsequent unloading, for the formation of disorientation bands. Figures 5; references 14.

UDC 539.18+539.145+539.2

Shock Waves a Quantum Effect?

907J0046B Novosibirsk FIZIKA GORENIYA I VZRYVA in Russian Vol 26 No 2, Mar-Apr 90 pp 138-140

[Article by Yu.N. Kuznetsov, Novosibirsk]

[Abstract] The effect of shock action on matter and particularly the response of a system of atoms to such a load are analyzed in the approximation of a linear Hugoniot curve, which is valid for many substances under gigapascal shock loads. Taken into account are motion of the nucleus, which determines the inertial characteristics of atoms, and attendant motion of an electron in accordance with the Bohr model. For illustration, consider a homogeneous metal in the ground state and a Wigner-Seitz atomic cell where the mean over "internal degrees of freedom" pseudopotential, representing the mean ground state energy, also characterizes the interaction of valence electrons and the atomic shell. One half of that energy being accordingly equal to the sum of ionization energy and bond energy, the contribution of each to the phase velocity of a perturbation propagating through matter upon high-pressure impact on the latter has been estimated for Be, Al, Ti, Fe, Cu, Mo, Ag, Ta, W, Au, Bi, by allowing quantization of the quasi-momentum $\Delta p = m\Delta u_0 = h/2a$ (u denoting the mass velocity, $a = 2r$ denoting the interatomic distance, r denoting the atomic radius). The estimated values of Δu_0 indicate a possible singularity of the atomic response, namely discrete motion in accordance with the law of momentum conservation and thus quantization of motion caused by a nonadiabatic perturbation. The phase velocity of a perturbation has been estimated on the basis of both Δu_0 and bond energy per atom $\Delta V_{0,mean}$, with the aid of available experimental data. Tables 1; references 10.

Dynamics of Acousto-Electromagnetic Waves in Crystals With Nonlinear Electrostriction

907J0073B Moscow ZHURNAL EKSPERIMENTALNOY I TEORETICHESKOY FIZIKI in Russian Vol 97 No 5, May 90 pp 1607-1615

[Article by G.N. Burlak, Kiev State University imeni T.G. Shevchenko]

[Abstract] Acousto-electromagnetic interaction in anisotropic crystals with nonlinear electrostriction as the interaction mechanism is analyzed, and the possibility of solitary envelope waves evolving, as a result, is demonstrated mathematically. A uniaxial crystal with 3m-symmetry is selected, in which two parallel electromagnetic waves, an ordinary one and an extraordinary one, propagating along the crystal x-axis interact with a transversely propagating acoustic wave. Linear electrostriction vanishes in this configuration so that quadratic electrostriction remains as first nonvanishing nonlinearly sound-dependent electrostriction mode. The system of corresponding equations of motion consist of four analogous Maxwell equations involving the $E_{y,z}$ components of the electric field vector in a transverse plane and the two diagonal components $\varepsilon_{1,3}$ of the permittivity tensor plus one equation of elasticity theory involving the three $g_{1,2,3}$ components of the electrostriction tensor renormalized so as to include the piezoelectric effect. The solution to this system of equation reveal amplification and high compression of a solitary envelope wave in the process of its evolution and subsequent propagation at a velocity of the order of the acoustic one. The results are applied to two characteristic cases of localized excitation and to encounter two oppositely traveling waves. In the absorption of sound, the crystal is taken into account when the interaction time tends to become infinitely long. Figures 4; references 17.

Generation of Strong Ultrasonic Pulses by Plane Surface or Concave Focusing Surface Exploded by Electric or Light Pulse

907J0074D Moscow PISMA V ZHURNAL EKSPERIMENTALNOY I TEORETICHESKOY FIZIKI in Russian Vol 51 No 11, 10 Jun 90 pp 586-590

[Article by G.A. Askaryan, M.G. Korolev, and A.V. Yurkin, Institute of General Physics, USSR Academy of Sciences]

[Abstract] An experimental study of ultrasonic sound emission by a plane surface in contact with a focusing lens and by a concave focusing surface during explosion

by electric or light pulses was made, ultrahigh-pressure pulses having been generated with kilobar amplitudes at the focus. A polyethylene terephthalate film with a solid metal or a metal powder coating for the electrical experiment and such a metallized film or layer of gouache for the optical experiment was inserted between the bottom of a cellulose triacetate beaker containing water and a plexiglass saucer. Both beaker bottom and saucer were either flat with a planoconcave acoustic lens placed on the beaker bottom inside or rounded with the downward-convex beaker bottom surface matching the upward-concave saucer surface. Electric pulses were generated by discharge of a 0.5 μF capacitor bank which had been charged through a 1 MΩ resistor to a voltage of 10 kV. Giant light pulses of up to 10 J energy and 40-50 ns duration were generated without focusing by a GOS-1001 Nd-laser with Q-switching by a self-clearing LiF shutter. The optical experiment was also performed on titanium foil, spherically cupped and coated with gouache or nitro dye, with the saucer replaced by a transparent film of nonmetallized polyethylene terephthalate, layer of glue, or layer of viscous gel on top of the foil inside the beaker. Electric explosions generate 2-4 μs sound pulses with a steep plane front and an amplitude of up to 300 atm at the surface, the amplitude becoming four times higher at the focus. Optical explosions generate pulses of up to 500 atm amplitude at the focus of the acoustic lenses, their focal length having been varied from 3 cm to 6.5 cm. These pulses were capable of shattering ceramic and rosin plates, the shattering becoming less localized as the focal length of the lens was increased. Figures 4; references 10.

Autowave of Spin Polarization in Semimagnetic Mixed-Phase Semiconductor

907J0007D Moscow PISMA V ZHURNAL EKSPERIMENTALNOY I TEORETICHESKOY FIZIKI in Russian Vol 51 No 5, 10 Mar 90 pp 268-271

[Article by Yu.G. Semenov and V.A. Stefanovich, Institute of Semicon- ductors, UkSSR Academy of Sciences]

[Abstract] Forming a dissipative structure with nonresonant optical bi- stability in semimagnetic mixed-phase semiconductor materials is considered, namely by injecting an amount of radiation approximately equal to the energy gap E_g and thus more is allowed in the equilibrium state, with an intensity sufficiently high for shifting the E_g edge of the fundamental absorption band in the "red" direction until the optical ab- sorption coefficient sharply increases. In cubic semimagnetic materials of the $A_{1-x}{}^2Mn_xB^6$ group, such a shift occurs owing to a change in the giant spin split of energy bands by an amount proportional to the dynamic polarization ΔP of localized spin moments, this change occurred due to exchange scattering of photoexcited holes by such moments. The general equation of kinetics for the polarization P of localized spin moments is derived from the system of equations for their dynamic polarization ΔP and for both polarization and concentration of photoexcited holes. In the case of a slowly varying P and fast varying subordinate hole polarization and concentration, assuming small diffusion length for holes, a closed partial differential equation for the rate of change of dynamic polarization is obtained which takes into account generation of spin-nonequilibrium electron-hole pairs as well as spin relaxation and spin diffusion. This equation has an autowave solution, provided the autowave remains inside the crystal, sufficiently far from both its front and back faces and its characteristic width is much smaller than the reciprocal of the Bouger-Lambert-Beer absorption coefficient. The authors thank S.M. Ryabchenko for discussions. Figures 3; references 3.

UDC 621.315.592

Optical Study of Kinetics of Germanium Crystal Vaporization by Laser Pulses

907J0015C Leningrad FIZIKA TVERDOGO TELA in Russian Vol 32, No 2, Feb 90 pp 548-558

[Article by M.Yu. Averyanova and S.Yu. Karpov, Institute of Engineering Physics imeni A.F. Ioffe, USSR Academy of Sciences, Leningrad]

[Abstract] An experimental study of crystalline and liquid germanium was made for a determination of changes in its optical properties during its vaporization by nanosecond laser pulses. Plate specimens of crystalline germanium grown by the Czochralski method with (100) or (111) orientation were mechanically polished and then heated by a beam of second-harmonic radiation (0.53 μm) from a Q-switched YAG:Nd^{3+} laser in pulses of 25 ns duration above half-amplitude, with a Gaussian distribution of energy density over the beam cross-section approximately 1.2 mm in diameter and with the mean energy density varied over the 20-500 mJ/cm^2 range. The surface of specimens was, during and after treatment, scanned with three beams 80 μm of a continuous-wave He-Ne laser carrying 0.63 μm, 1.15 μm, 3.39 μ radiation respectively and incident at a 20° angle, each beam being approximately 0.08 mm in diameter. In order to minimize interference during probing with 3.39 μm radiation, to which crystalline germanium is transparent, it was necessary to put a dull finish on the back surface before treatment. The reflection coefficient of germanium for each probing radiation was found to vary in time, passing through a maximum and a minimum at instants depending on the energy density and its dependence on that energy density following a similar trend for each probing radiation. With the aid of these experimental data,both the melting point and the heat of fusion is pinpointed, which was needed for evaluating the optical properties of crystalline germanium heated by nanosecond laser pulses and of germanium melt produced by such a treatment. The accuracy of this analysis, which depends largely on the degree of superheating prior to melting, is estimated by considering the nonlinearity of the temperature dependence of the reflection coefficient as well as interference of probing radiation in a nonuniformly heated surface layer. The latter effect is evaluated on the basis of a numerical simulation which takes into account the nonmonotonic temperature dependence of dielectric permittivity and using different mathematical models of its depthwise profile in a semiconductor treated with 0.63 μm and 1.15 μm radiation respectively. While the esti- mated superheating is 200-400 K on the basis of probing with 0.63 μm radia- tion. Its estimation, based on probing with 1.15 μm radiation, is unreliable, inasmuch as correctly accounting for the intricate interference effects in this case is very difficult. The authors thank V.Ye. Myachin and I.A. Sokolov for assisting in the experiment, Yu.V. Kovalchuk and Yu.V. Pogorelskiy for discussion of the results. Figures 5; tables 2; references 20.

Feasibility of Determining Electronic Structure of Impurities at Dislocations by Optical Methods

907J0049A Leningrad PISMA V ZHURNAL TEKHNICHESKOY FIZIKI in Russian Vol 16 No 5, 12 Mar 90 pp 71-75

[Article by M.V. Goldfarb and M.I. Molotskiy, Voronezh State University]

[Abstract] A model of the electronic structure of a donor impurity at dislocations in a host semiconductor has been proposed by the authors in which the impurity atoms are situated on dislocation axes but at a distance of the order of the lattice constant from them. Inasmuch as the affinity of an electron to a dislocation here is at least one order of magnitude higher than the donor ionization potential, a donor electron will become

pinned to a broken dislocation bond and will not rejoin a donor nucleus situated in an accessory half-plane. Accordingly, it should be possible to control the electronic characteristics of crystals by controlled deposition of impurities. On the basis of this model, the feasibility of such a control with optical monitoring is now theoretically demonstrated, the absorption spectra shown to contain the necessary information about radiation absorption by dislocations attending transitions of electrons from bound states to states within the conduction band. A typical case is a phosphorus impurity in a silicon crystal, the donor level of this impurity lying 0.16 eV below the bottom of the dislocation band. The authors thank K.A. Kikoin and V.Ya. Kravchenko for constructive discussion. Figures 1; references 10.

UDC 621.315.592

Dynamics of Photoinduced Diffraction Gratings in Silicon During Excitation by Picosecond Pulses

907J0050A Tomsk IZVESTIYA VYSSHIKH UCHEBNYKH ZAVEDENIY: FIZIKA in Russian Vol 33 No 3, Mar 90 pp 53-58

[Article by N.A. Kudryashov, S.S. Kucherenko, Ye.A. Mazur, A.N. Petrovskiy, and M.P. Yakovlev, Moscow Institute of Engineering Physics]

[Abstract] The method of dynamic diffraction gratings in semiconductors is applied to a theoretical and numerical analysis of excess charge carrier generation and relaxation or in such a semiconductor, considering excitation of the semiconductor and formation of a grating by coherent picosecond light pulses of the same intensity interfering inside the material. The two processes are described by two partial differential equations for the rates of change of electron and hole concentration respectively in the one-dimensional approximation. Each rate of change of concentration is equal to the rate of charge carrier generation minus the rate of their recombination plus the rate of their respective diffusion dependent on their respective mobility as well as on the dielectric permittivity of the material. The results of analysis and calculations are compared with experimental data, a 300 μm thick specimen of KEF-500 n-silicon with electron concentrations up to 10^{13} cm^{-3} having been excited with a beam of 1.06 μm light from a glass:Nd^{3+} laser in pulses of approximately 8 ps duration. Diffraction of this light was monitored by means of a light beam focused 2.5 times more sharply than the exciting one, to ensure its falling into uniformly excited spots within a nonuniform diffraction grating, recorded in such a thick specimen. Figures 4; references 11.

UDC 621.315.592

Electrophysical Properties of Epitaxial CdTe Films

907J0050B Tomsk IZVESTIYA VYSSHIKH UCHEBNYKH ZAVEDENIY: FIZIKA in Russian Vol 33 No 3, Mar 90 pp 72-76

[Article by A.P. Belyayev, V.P. Rubets, and I.P. Kalinkin, Leningrad Institute of Technology imeni Lensovet]

[Abstract] An experimental study of epitaxial CdTe films was made for a determination of its electrophysical properties depending on the technology of their deposition, 2-4 μm thick films were deposited on muscovite substrates at 450-650°C temperatures: some in a quasi-closed vessel and some with a thermal shield. Gold contacts were deposited on them for measurement of the Hall effect, the electrical conductivity, and the thermo-e.m.f. within the ohmic range of the current-voltage characteristic over the 120-410 K temperature range. Much has been determined on the basis of this data, such as, the Hall mobility, the mobility activation energy and the conductivity activation energy, then the amplitude of the random potential characterizing a nonhomogeneous semiconductor and in all cases found to be approximately 0.21-0.23 eV at all temperatures, also the Mott temperature and with it the density of states at the Fermi level. The results indicate that epitaxial CdTe films produced by both methods are semiconductors with nonuniform potential profiles of energy bands. Films produced in a quasi-closed vessel are more defective than those produced with a thermal shield and at higher temperatures, their electrical conductivity jumps irregularly. Figures 4; tables 1; references 8.

Density Matrices for Superfluid Helium-4, Part 2

907J0009B Moscow TEORETICHESKAYA I MATEMATICHESKAYA FIZIKA in Russian Vol 82 No 3, Mar 90 pp 438-448

[Article by I.A. Vakarchuk, Lvov State University]

[Abstract] The s-particle density matrix for the ground state of a system of interacting Bose particles, having been calculated in Part 1, with not only a pair but also three-particle and four-particle correlations included, the pair distribution function is now put in classical form with a mean-force potential and the one-particle density matrix then expressed in terms of the liquid-phase structural parameter S_q for application to a Bose condensate. The relative number of atoms N_0/N in a Bose condensate at temperatures covering the 1.0-4.27 K range from 1.0 K to 4.2 K has been calculated earlier in both first and second approximations for helium-4 containing such a condensate. From energy calculations are now derived two expressions, the one for the average kinetic energy being quite simple and the one for the average potential energy being more intricate. The equation of state is derived next in the first approximation, the pressure being obtained from the ground-state energy, for a quantitative evaluation of parameters characterizing the super-fluidity of helium-4. Theoretical calculations on the basis of S_q values, obtained by measurement in diffraction experiments, yield for helium-4 at T = 0 K temperature an internal energy of -6.4 K/atom, an average kinetic energy of 14.2 K/atom, an average potential energy of 20.6 K/atom, and 3.7% atoms in the Bose condensate. The author thanks G.V. Bugriy, P.A. Glushak, and V.M. Migal for computer-aided calculations. Tables 1; references 32.

Ginzburg Criterion and Equation of State for Metastable Liquids

907J0014B Moscow ZHURNAL EKSPERIMENTALNOY I TEORETICHESKOY FIZIKI in Russian Vol 97, No 3, Mar 90 pp 842-85

[Article by V.G. Boyko, Institute of Surface Chemistry, UkSSR Academy of Sciences, V.M. Sysoyev, Kiev State University imeni T.G. Shevchenko, and A.V. Chalyy, Kiev Institute of Medicine imeni A.A. Bogomolets]

[Abstract] Physical properties of metastable systems at various degrees of intrusion into the metastable state and in various parts of the metastable region are analyzed from the standpoint of the fluctuation criterion which describes this region and is analogous to the Ginzburg-Levanyuk criterion, describing phase transitions of the second kind in the self-consistent field theory. A one-component liquid at a constant temperature is considered the basic model, such system being in a metastable state along a segment of any subcritical isotherm which passes through a point on the binodal line of liquid-vapor coexistence. The condition for such a system to still retain its thermodynamic stability during nucleation of the new phase is the inequality $R_{min}/k_BT > X$ (R_{min} denotes the minimum work needed for a nucleus of the new phase to grow to critical dimensions, k_B is the Boltzmann constant, T is the absolute temperature, X is a dimensionless constant, larger than 100, for vapor bubbles during evaporation and equal to 60 for liquid droplets during condensation). Within the meta- stable region the density does not fluctuate when R_{min}/k_B TX is much larger than 1 and does fluctuate when R_{min}/k_BTX is much smaller than 1. Examination of the fluctuationless metastable state on the basis of the Landau-Lifshits relation for R_{min} applied to spherical nuclei takes into consideration the dependence of this minimum work on the coefficient of surface tension as well as on the density relative to that of the original phase and on the pressure relative to that on the binodal line, the pressure being in turn both density and temperature dependent. With pressure as well as density and temperature normalized to their respective critical ones, an equation of state in the fluctuationless metastable region is derived on the basis of that relation. The specific volume v, the excess pressure $p-p_0$, and the derivative $-(\delta/dv)_T$, calculated according to this theory for water vapor on the T = 260°C isotherm (saturation pressure 4.694 MPa) and on the T = 300°C isotherm (saturation pressure 8.592 MPa), also for argon on the T = 125 K isotherm (saturation pressure 1.5812 MPa) agree closely with those obtained by extrapolation of experimental data pertaining to the stable region of both substances, which indicates extrapolation of isotherms from the stable region into the fluctuationless metastable one is permissible. Extrapolation into the region about the critical point, where fluctuations take place, is not permissible, because here the system is not symmetric as it is in the fluctuationless region with respect to change of scale of space variables so that an asymmetric scale equation of state is needed. The evolution of the new phase in the form of growing spherical nuclei has revealed their fractal nature. The concept of codimensionality and interpretation of transversality, from that standpoint, is essential for a meaningful analysis of their dimen- sional diversity. Figures 2; tables 1; references 18.

UDC 536.24

Identification of Characteristics of Thermal Interaction of Materials With Gas Streams

907J0054B Moscow TEPLOFIZIKA VYSOKIKH TEMPERATUR in Russian Vol 28 No 2, Mar-Apr 90 pp 323-330

[Article by Ye.A. Artyukhin and A.V. Nenarokomov, Moscow Institute of Aviation imeni S. Ordzhonikidze]

[Abstract] Breakdown of surfaces of materials by thermal interaction with gas streams which specifically changes its emissivity is considered, determination of the characteristics of such a breakdown being treated as an inverse problem of heat transfer. A unique solution to this problem is obtained by performing L different experiments with specimens of the same material under

nonstationary conditions, the number L being equal to or larger than the number of sought characteristics K, and then simultaneously processing all the data. The procedure is based on the equation of transient heat transfer $c(T)gdT_l/\delta t = \delta(\lambda(T)T_l/\delta x)/\delta x)$, where l = [begin set]1,L[end set], temperature $T_l = T_l(x,\delta t)$, $\lambda(T)$ and c(T) are the temperature-dependent thermal conductivity and volumetric specific heat of the material, and x is the depth of erosion dependent on the mass rate of wear $G_{w,l}(\tau)$, the latter being a function of time τ and of the temperature-dependent density $\rho(T)$ of the material. The solution to this equation for the appropriate initial and boundary conditions is sought in the class $C^{0,2}$, the unknown emissivity and thermal flux as functions of the surface temperature T_w being approximated with cubic B-splines. The inverse problem of heat transfer is then treated as a minimization problem and solved by a special gradient method. The entire procedure is demonstrated on a thermophysically homogeneous multilayer plate with ideal thermal contact between layers and with thermometers or thermocouples at its boundaries. There follows an accuracy analysis in which errors of calculations based on readings of two instruments are compared with errors of calculations based on readings of four instruments and the dependence of errors in the calculated thermal interaction characteristics on the measurement errors is estimated. A test of this method for possible redundancy of experiments, besides indeterminacy due to a redundancy of temperature measurements in each experiment, indicates that supplementing two experiments with a third one does not improve the accuracy of the results, inasmuch as only two out of three yield the best data. Figures 2; tables 4; references 7.

Superfluidity in Systems with Fermion Condensate

907J0055B Moscow PISMA V ZHURNAL EKSPERIMENTALNOY I TEORETICHESKOY FIZIKI in Russian Vol 51 No 9, 10 May 90 pp 488-490

[Article by V.A. Khodel, Institute of Atomic Energy imeni I.V. Kurchatov, and V.R. Shaginyan, Institute of Nuclear Physics imeni V.P. Konstantinov, USSR Academy of Sciences]

[Abstract] The behavior of a Landau Fermi-liquid beyond the phase transition point is analyzed, the three distinguishing characteristics of such a system being a step in the momentum distribution of particles at the Fermi momentum point, a linear temperature dependence of the specific heat as the temperature approaches zero, and a logarithmically increasing amplitude of scattering, at the Fermi surface, of quasiparticles with zero resultant momentum. The necessary condition for validation of the Fermi-liquid theory is shown to be a non-negative group velocity of quasiparticles on the Fermi surface. The behavior of a system of 'heavy' fermions, a system with a fermion condensate, by analogy, to a Bose liquid, is analyzed on the basis of a simple model with a phenomenological effective functional. The problem is finding the optimum momentum distribution of a given number of such particles interacting with a known pairing potential in an elastic external field and with the electron concentration necessarily nowhere higher than the critical one $1/4\pi^3$. The solution is utterly simple in the case of "Coulomb" interaction. Immediately beyond the transition point, according to this model, the condensate contains all particles simultaneously and the step in their momentum distribution remains, but shifts to a point higher than the Fermi momentum point. Following determination of the ground state on this basis, the latter is analyzed for stability. Its multiple degeneracy is shown to result in violation of some conditions for its stability, as in the case of a predominant singlet pairing instability associated with attractive interaction between condensate particles and their attendant formation of Cooper pairs. The authors thank S.T. Belyayev, V.G. Zelevinskiy, and S.V. Tolokonnikov for discussion. References 5.

UDC 532.614

Photoinduced Changes in Surface Energy of Amorphous As-Se Films

907J0065A Riga IZVESTIYA AKADEMII NAUK LATVIYSKOY SSR: SERIYA FIZICHESKIKH I TEKHNICHESKIKH NAUK in Russian No 2, Mar-Apr 90 pp 17-20

[Article by Ya.A. Teteris, K.I. Grebreder, and V.I. Gerbreder, Institute of Physics, LaSSR Academy of Sciences, and Daugavpils Pedagogical Institute]

[Abstract] An experimental study of amorphous thin As-Se films was made concerning the relation between their optical properties and their surface energy, stoichiometric $As_{0.4}Se_{0.6}$ films and $As_{0.5}Se_{0.5}$ one with excess As having been deposited on transparent substrates by vapor condensation under vacuum and then annealed in air at a temperature near the respective glass transition point. They were illuminated through the substrate with 632.8 nm light of 0.1 W/cm^2 intensity from a He-Ne laser at 20°C temperature. The surface energy was determined indirectly on the basis of the contact angle with a drop of glycerin in air. This angle was measured on the image on a screen with an error not exceeding +/- 1.5°, whereupon the surface tension was calculated according to the Young equation and the adhesion work was calculated according to Young-Dupré. Measurements were made on fresh films and on annealed ones. The results reveal that light and, to a lesser extent, heat increase both the surface tension and the adhesion work, the magnitudes of the increments depending on the film composition and being much larger on films with excess As. The surface tension on fresh stoichiometric films in air was found to first increase and then slowly decrease. Figures 2; references 5.

UDC 537.523.5

Laws Governing Combustion of Titanium Particles in Gas Streams

907J0065C Riga IZVESTIYA AKADEMII NAUK LATVIYSKOY SSR: SERIYA FIZICHESKIKH I TEKHNICHESKIKH NAUK in Russian No 2, Mar-Apr 90 pp 106-113

[Article by A.P. Dolganov, V.N. Kovalev, V.E. Liepina, and Ye.I. Shipin, Institute of Physics, LaSSR Academy of Sciences]

[Abstract] An original experimental study was made concerning combustion of loose metal particles in hot gas streams of controllable composition. The apparatus consisted of a plasmatron, an electric-arc gas preheater, a mixing chamber, a powder batcher, a tubular instrument channel, and a system of gas, water, and electric power supply, including tanks and distributors with level control, also an an oxygen tank and an argon tank. The experiment was performed with titanium powder fed into the gas stream at rates of 0.001-1.0 g/s. The instrument channel, 4 cm in diameter and 50 cm long, was installed in segments of various lengths inside the mixing chamber with windows between segments for visualization and measurements. The temperature of the gas mixture at the entrance to the instrument channel varied around the 3000-4000 K range, depending on the mode of plasmatron operation. The experiment was set up to prevent interaction of burning particles with one another in the gas stream and to minimize the effect of particles on the gas stream. Accordingly, radial and axial temperature profiles in the gas stream alone were measured first, prior to injection of sparse powder particles for tracking and measurement of their temperature, velocity, concentration, and size distribution along their tracks. Particles were sampled from the gas stream at various stages of their combustion through successive taps in the channel, for phase and dispersion analyses of the residue (Ti + titanium oxides). Temperature measurements were made with Pt/(Pt-Rh) thermocouples. The composition of the gas mixture and the distribution of oxygen in the gas stream were monitored with the aid of an MI-5130 analyzer. Phase analysis was performed in a DRON-3 x-ray diffractometer. Photographs were taken and the size distribution of particles was plotted under an optical microscope with a MORFOQUANT apparatus. The results indicate that combustion of polydisperse Ti powder, under such conditions, produces many ultrafine-disperse TiO_2 grains, mostly of anatase, some coarse grains of rutile, and also black particles of Ti_nO_{2n-1} oxides where combustion is incomplete. The study has yielded a wealth of preliminary data on the kinetics and the intricate mechanisms of metal powder combustion. Figures 5; references 13.

W-Bosons and Structure of A-B Interface in Superfluid He-3 Under Low Pressure

907J0069B Moscow ZHURNAL EKSPERIMENTALNOY I TEORETICHESKOY FIZIKI in Russian Vol 97 No 4, Apr 90 pp 1198-1207

[Article by G.Ye. Volovik, Institute of Theoretical Physics imeni L.D. Landau, USSR Academy of Sciences]

[Abstract] The structure and the dynamics of the A-phase (He-3) and B-phase (He-4) interface in superfluid He-3 under low pressure are analyzed in the approximation of weak interaction, considering that under low pressure the low-temperature A-phase can exist only in a strong magnetic field. Domain walls are shown to expand under these low-temperature, low-pressure conditions because of two factors exactly analogous to phenomena involving elementary particles, namely the existence of collective boson fields corresponding to W-boson fields in electro-weak interaction theory and the zero-charge effect known in quantum electrodynamics. An exponentially asymptotic behavior of four collective W-boson modes in the A-phase is established on the basis of their Lagrangian and the Bogolyubov equation, maximally symmetric A-B interfaces, most relevant here, and the corresponding five components of the order parameter evaluated accordingly. Domain walls with broken symmetry are considered next, weakening of the magnetic field or approximate degeneracy between the A-phase and the planar phase are sufficient to break their symmetry under low pressure and thus during weak interaction. A nonnumeric hypothetical phase diagram for the A-B interface is plotted in the H-P (magnetic field pressure) plane on the basis of the proposed theory. The author thanks M.M. Salomaa and N. Schopohl. Figures 3; references 18.

Generation of a Cyclonic Vortex or Laboratory Model of Tropical Cyclone

907J0074A Moscow PISMA V ZHURNAL EKSPERIMENTALNOY I TEORETICHESKOY FIZIKI in Russian Vol 51 No 11, 10 Jun 90 pp 557-559

[Article by G.P. Bogatyrev, Perm State University imeni A.M. Gorkiy]

[Abstract] A tropical cyclone and its distinctive feature, namely interaction of large-scale advective flow and Coriolis forces during ascent of an air stream within the center core, were simulated in the laboratory with a cylindrical cell 300 mm in diameter made of plexiglass containing a 30 mm high column of fluid and rotating about its vertical axis. While its angular velocity varied around the 0.002-0.4 s^{-1} range, the angular velocity of the fluid within the center core was measured with a floating transducer. The latter was measured by three cylindrical plexiglass beakers 10 mm in diameter spaced 120° apart around a circle 15 mm from the axis of the cell and clearing the bottom of the cell by about 0.5 mm. The fluid was heated by an electric brass plate 105 mm in diameter at the center of the bottom of the cell. It was

heated at a steady rate, the power being regulated to vary the temperature drop across the height of the fluid column over the 2-35°C range. With the cell at rest, heating of the fluid produced three convection patterns: 1) advective flow due to the radial temperature gradient, including average ascent above the heater, divergent flow with natural heat dissipation, descent along the wall, and convergent flow near the bottom; 2) steady flow of randomly buoying hot streaks; 3) convective flow of billows outside the heating zone, their axes tending to become radially oriented. Rotation of the fluid was found to give rise to interaction of convection forces and Coriolis forces with an attendant evolution of a spiral vortex isolated from the region of advective flow. The experiment was performed with two fluids having quite different Prandtl numbers: pure transformer oil and 2:1 mixture of transformer oil with kerosene. Measurements have yielded the rate of vortex intensity rises with increasing Grashof number, the rate depending on the Reynolds number and being much higher when the latter is 105 than when the latter is 7. The critical Grashof number is not dependent on the Prandtl number but is dependent on the Reynolds number. As the latter was increased 7 to 140, the critical Grashof number first quickly decreased from about 95,000 to about 16,000 at a Reynolds number of about 12 and then to rise again but slower to about 125,000. The results are qualitatively consistent with data on tropical cyclones developing within the 5-30° zone, especially between 10° and 15° latitudes whenever the Reynolds number is optimum corresponding to the minimum vertical temperature drop. Figures 3; references 3.

Analysis of Lasing of Al_2O_3:Ti^{3+} Laser With Synchronous Pumping by Limited Ultrashort-Pulse Train

907j0033a Minsk Zhurnal Prikladnoy Spektroskopii in Russian, Vol 52 No 3, Mar 90 pp 381-387

[Article by R. G. Zaporozhchenko, I. V. Pilipovich, A. V. Kachinskiy, and V. D. Asimova, Institute of Physics imeni B. I. Stepanov, Belorussian Academy of Sciences, Minsk]

[Text]The authors of[1] demonstrated the use of the new laser medium Al_2O_3:Ti^{3+} to produce tunable operation at 700-1000 nm with coherent pumping. Various modes of lasing have now been achieved in Al_2O_3:Ti^{3+} with lamp, coherent pulse and continuous pumping.[1-6]. The spectroscopic properties of the new medium have been intensely studied. Analysis of the latest studies on sapphire with Ti^{3+}[7-10] has shown that the main problem preventing extensive application of this laser medium is the lack of a mature technology for the growth of crystals with predetermined and reproducible characteristics. One important problem continues to be the determination of the concentration of trivalent titanium ions participating in processes of absorption of pumping and lasing, contained in the lattice with octahedral symmetry, since titanium can occupy a position in the lattice with tetrahedral symmetry and may be present as Ti^{4+} in the structure of the sapphire. Determination of their relative concentrations is a difficult spectroscopic problem.

The purpose of this work was to study lasing in an Al_2O_3:Ti^{3+} crystal upon synchronous pumping by a train of picosecond pulses, the second harmonic of an yttrium-aluminum garnet laser, by mathematical modelling of the process and comparison of its results with the experimental data.

Calculations were performed for the experimental system shown in Figure 1a. The pumping radiation, a train with a sine-wave envelope, was directed toward the Al_2O_3:Ti^{3+} crystal which was placed in a resonator synchronously tuned to the period of the pumping train.

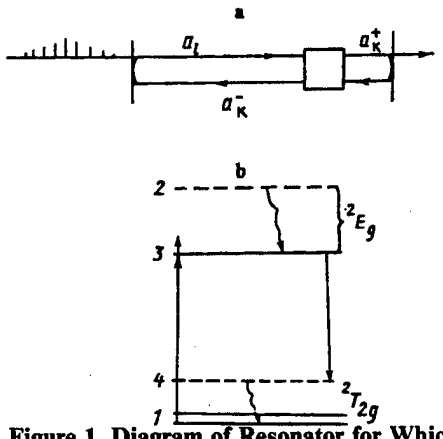

Figure 1. Diagram of Resonator for Which Calculations Were Performed (a) and Electronic Oscillating System of Levels in Crystal Al_2O_3:Ti^{3+} (b)

In the generally accepted diagram of the levels of sapphire with titanium[2] [(Figure 1b)], there are no transitions to the upper excited states, and therefore the dynamics of population of the levels can be described by a four-level model. The pumping pulses had length τ_i much greater than T_2, where T_2 is the time of phase relaxation of the medium; therefore, the change in polarization was not computed, and in the quasi-steady approximation, the dynamics of population of levels n_i, pumping fields A_l, and lasing are described by the equations

$$\frac{dn_1}{dt} = \gamma_1 n_4 - \alpha a_l^2 (n_1 - n_2), \tag{1a}$$

$$\frac{dn_2}{dt} = \alpha a_l^2 (n_1 - n_2) - \gamma_2 n_2, \tag{1b}$$

$$\frac{dn_3}{dt} = -\beta (a_K^{+2} + a_K^{-2})(n_3 - n_4) + \gamma_2 n_2 - k_3 n_3, \tag{1c}$$

$$n_4 = 1 - (n_1 + n_2 + n_3), \tag{1d}$$

$$\frac{\sqrt{\varepsilon_l}}{c}\frac{\partial a_l}{\partial t} + \frac{\partial a_l}{\partial z} = -g_l a_l (n_1 - n_2) - g a_l, \tag{1e}$$

$$\frac{\sqrt{\varepsilon_K}}{c}\frac{\partial a_K^{\pm}}{\partial t} \pm \frac{\partial a_K^{\pm}}{\partial z} = g_K a_K^{\pm} (n_3 - n_4) + \sigma_{cn} n_3. \tag{1f}$$

Here γ_1 and γ_2 are the widths of the levels $^2T_{2g}$ and ^2E_g, respectively;

$$\alpha = \frac{\sigma_{em}}{\hbar\omega_l} \times \frac{2\pi}{c};\ \beta = \frac{\sigma_{ex}}{\hbar\omega_K}\frac{2\pi}{c};\ \sigma_{em},\ \sigma_{ex},\ \sigma_{cn}$$

are the absorption, emission and spontaneous emission cross sections; ω_l, ω_k are the pumping and lasing frequencies;

$$\sigma_{cn} = \frac{\hbar\omega_K k_3 N}{4\pi}\Delta\Omega;\ \Delta\Omega$$

is the solid angle; $k_3 = T^{-1}{}_1$, T_1 is the luminescence life time; $\varepsilon_{l,k}$ is the dielectric constant at frequencies ω_l, ω_k; $g_l = \sigma_{em}N/2$; $g_k = \sigma_{ex}N/2$; g are the nonresonant pumping radiation losses; N is the concentration of active Ti^{3+} particles.

The problem was solved for the following initial and boundary conditions

$$n_1(t=0) = N,\ n_i = 0,\ i = 2-4,$$

$$a_K^{\pm}(t=0,\ z) = 0,$$

$$a_l = a_l^0 \sum_{m=1}^{M} \sin(\pi m/M) \exp\left\{-4\ln 2\left(\frac{t-t_0}{\tau_u}\right)^2\right\}, \tag{2}$$

$$a_K^+(t,\ z=0) = R_1 a_K^-(t,\ z=0),$$

$$a_K^-(t,\ z=L_{on}) = R_2 a_K^+(t,\ z=L_{on}),$$

where m is the number of the current pulse; M is the total number of pulses in the train; τ_u is the length of a pumping pulse; L_{on} is the optical length of the resonator;

R_1 and R_2 are the reflectances of the resonator mirrors for the field amplitudes of frequency ω_k.

The selection of parameters for the calculations was based on data obtained in preliminary experiments on synchronous pumping of a laser based on an $Al_2O_3:Ti^{3+}$ crystal 2.8 cm in length. The initial value of amplitude a^0_1 of the maximum pulse in the train was selected based on conditions under which the total pumping energy of the train did not exceed 10 mJ, which was close to the threshold of failure of the active medium of $Al_2O_3:Ti^{3+}$. The pulses in a train had equal length τ_u = 100 ps, their number varying from 9 to 15; R_1 = 1, R_2 = 0.84. In the calculations, lasing was developed from spontaneous noise described by the term $\sigma_{on}n_3$ in equation (1e), and the preferential direction was considered to be the direction in which the pumping propagates. This assumption follows from the experimental conditions, where the crystal was located near one of the mirrors, and therefore the superluminescence gained conditions that were asymmetrical and lasing developed in one direction (as in.[5]) The difference in the data from the literature on parameter σ_{em}, σ_{ex} made their adequate determination difficult. Thus, the values of the parameters σ_{em}, σ_{ex}, T_1, according to [1, 4, 7-9] falls within the bands $(0.5\text{-}1)\cdot10^{-19}$ cm^2, $(1.7\text{-}3.3)\cdot10^{-19}$ cm^2, $(2.4\text{-}4)\cdot10^{-6}$ x, T_2 is approximately 10^{-13} s.

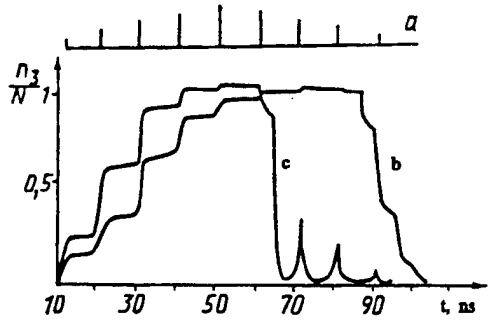

Figure 2. Shape of Pumping Train (a) and dynamics of level n_3/N with time for maximum pulse intensity in pumping train; 1 (b) and 43 GW/cm^2 (c)

The experimental data which we obtained plus the data presented in[5] have shown that the efficiency of ultrashort pulse lasing in $Al_2O_3:Ti^{3+}$ in picosecond excitation mode is 5-10 percent, while the pumping absorption for various crystals is 75 to 95 percent. A comparison of these figures with the numerical estimates of lasing intensity and pumping for various N, σ_{em}, σ_{ex} and g = 0 has shown that the calculations must consider nonresonant losses in the pumping channel, since where g = 0, 95 percent pumping absorption is not achieved with any realistic values of the parameters σ_{em}, N and a_l^0. This apparently indicates the presence in real crystals of certain pumping energy loss mechanisms, some of which are discussed below.

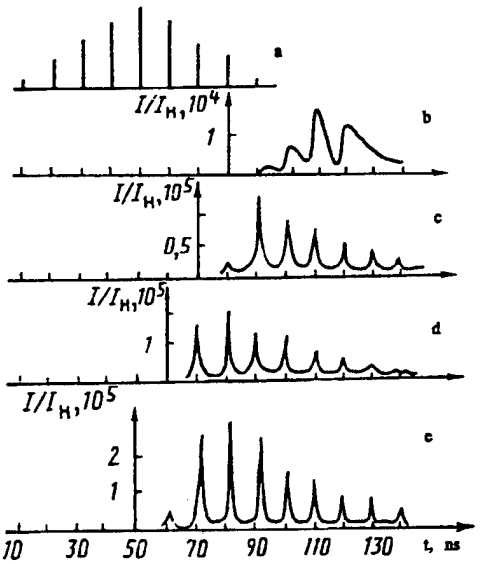

Figure 3. Time Envelopes of Pumping Trains (a) and Lasing for Various Pumping Intensities: 1(b), 24 (c), 43(d) and 67 GW/cm^2 (e)

The results of calculations presented in Figures 2-4 were obtained with the following parameters: $\sigma_{em} = 0.5\cdot10^{-19}$ cm^2, $\sigma_{ex} = 3\cdot10^{-19}$ cm^2, $N = 0.2\cdot10^{19}$ cm^3, $g_l+g = 1.3$ cm^{-1}, g is congruent with $2g_l$, pumping amplitude a_l^0 was varied. Figure 2 shows the dynamics of the change in population of the working level with time for various pumping intensities, while Figure 3 shows the shape of the pumping trains and generation for various excitation levels. Figure 4 shows the variation of quantitative lasing pulse characteristics. At low excitation levels (Figure 2b, 3b), the threshold inverted population is achieved in the tail of the pumping train and the stored energy is released as a pulse about 50 ns in length with strong sawtooth modulation. As pumping intensity increases, the depth of gain modulation increases, and when the threshold is exceeded by a factor of two, the maximum value of n_3 is reached after the fourth pumping pulse (Figure 2c), while the laser radiation is a train of seven or eight short pulses (Figure 3c). Further increases in pumping intensity, as Figure 3 shows, shift the beginning of lasing to the center of the pumping train and reduce the length of the pulses generated. Figure 3d corresponds to intensities approximately twice as great as those achieved in our experiments and corresponding to the threshold of failure of the specimen.

As we can see from Figure 4, the maximum efficiency of generation η = 40% (η is the ratio of the total energy of all laser pulses to the energy of the pumping train), achieved near the threshold for sawtooth laser pulses (Figure 2b,

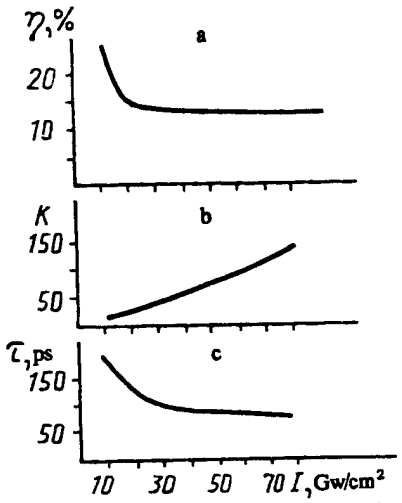

Figure 4. Variation in Effectiveness of Lasing η (a), Radiation Contrast *K* (b), Length of Generated Pulse (c) with Pumping Intensity

3b). As pumping increases, upon transition to generation of an ultrashort pulse train, η decreases and stabilizes at a value of about 12 percent. Here the contrast *K* (*K* is the ratio of intensity at the maximum to the mean intensity between neighboring pulses) increases significantly, while the length of a single pulse decreases to 80 ps.

A study of the output characteristics of lasing as a function of resonator parameters showed that as the reflectance of the second mirror R_2 changes (Figure 1b), these characteristics change little. Thus, varying R_2 between 0.7 and 0.9 caused a change in η of only one percent, while the change in pulse length was still less, which agrees with the experimental data of.[3, 5] An important factor influencing the ultrashort pulse parameters is detuning the length of the resonators $\Delta L = L_k - L_l$ of the sapphire plus titanium lasers and pumping. With pumping corresponding to Figure 3d, optimal detuning was found to be 1.5 mm. As ΔL increased, the shape of the pulses was distorted and their length increased, the background between pulses rose, along with the lasing efficiency. Thus, where ΔL is plus or minus 2.5 mm the length of the pulses is 250 ps and they take on additional modulation.

The results of calculation presented above agree qualitatively with the experimental data on an $Al_2O_3:Ti^{3+}$ laser with synchronous pumping by an ultrashort pulse train, the second harmonic of a YAG:Nd^{3+} laser with active-passive mode synchronization. The active medium used was an element of sapphire with titanium and diameter of 7x28 mm, placed in a linear resonator formed of flat and concave (r = 2.5 m) mirrors with reflectances of 75 and 99 percent in the 700-800 mm area. Synchronous pumping of the $Al_2O_3:Ti^{3+}$ was performed by the radiation of the second harmonic of a YAG:Nd laser with active-passive mode synchronization and two-stage amplification. A train pumps 9-12 pulses with a length of about 100 ps and energy up to 10 mJ through the concave mirror of the resonator (transparent to the pumping) by means of a spherical lens with a focal length of 1.3 m focused near the far end of the active element. The length of the laser resonator was tuned to resonance with the optical length of the pumping laser resonator.

During the process of the studies, the energy and time characteristics of the laser radiation were recorded. The time characteristics of the ultrashort pulses were measured with a type FK-26 element and a high-speed type S7-19 oscilloscope. Figure 5 shows oscillograms of the pumping train (Figure 5a) and the generation of the $Al_2O_3:Ti^{3+}$ laser (Figure 5b-d) at various excitation levels. At near-threshold conditions $W_p = 1.1\ W^t_p$ (W^t_p is the threshold pumping energy), the radiation produced was a sawtooth pulse 80 ns in length (Figure 5b). As pumping increased, the depth of modulation of the envelope increased and the time profile was transformed to a train of short pulses (Figure 5c, $W_p = 1.5\ W^t_p$). With pumping at W_p = 10 mJ, corresponding to twice the threshold (Figure 5d), the pulses generated had lengths of about 250 ps, the efficiency was about 5 percent. A comparison of Figures 3 and 5 indicates good qualitative agreement of the numerical calculations and experimental data.

Caption: Figure 5. Envelopes of Pumping (a) and Lasing (b-d) Pulse Trains. [Figure not reproduced]

We should note that the model described by equations (1) does not consider spatial heterogeneity of the medium, or the radiation, or residual absorption at the lasing frequency. As was shown in[10, 11] the residual IR absorption may vary from 0.001 to 0.15 times the maximum gain depending on the crystal growth conditions. Special measurements of this quantity were not performed. According to approximate estimates, these losses are at least an order of magnitude less than the gain. An attempt was made to consider this absorption in the calculations by introducing the loss factor at the laser frequency to equation (1e). The computations showed that the value of these losses significantly influences the development time, length of ultrashort pulses and lasing efficiency.

We also calculated the synchronous pumping mode in $Al_2O_3:Ti^{3+}$ crystals for shorter pumping pulses (τ_u = 25 ps). For the radiation parameters presented in[5] (where the parameters of the crystal are not reported) at the absorption cross sections, gain selected and a crystal length of 2.8 cm, the time parameters of the ultrashort pulses formed, repeated the parameters of the pumping pulses, while the lasing development time decreased in comparison to the data presented in Figure 3, due to the great intensity of excitation (up to 100 MW/cm^2). This result contradicts the experimental fact observed in[5], showing that in these radiation parameters, a delay was observed in the development of lasing in the $Al_2O_3:Ti^{3+}$ crystal of up to 300 ns. We attempted to analyze possible causes of this effect.

Within the framework of the computation model suggested, described by equations (1), it is assumed that the characteristic parameters of the medium and relaxation time T_1, T_2 are constants. However, we should note that in[5] the radiation intensity was up to 100 GW/cmU2O, corresponding to field amplitudes of a_l^0 of about $3 \cdot 10^8$V/m. Such fields may disrupt the processes of relaxation in the bands $^2E_{2g}$ and $^2T_2$, "gaps" may arise as a result of the interaction of the radiation with phonons and electrons, and correlation may be established between the lower and upper states of the electron-oscillating system[12]. This may lead to a delay in relaxation and coherent interaction of pumping with the medium, causing a delay in the formation of the laser pulse. However, this mechanism cannot explain a lasing development time of about 300 ns without considering other effects in the crystal.

In[13], stepped transitions to other states of $Al_2O_{3:Ti^{3+}}$ were experimentally detected, dependent on the intensity of excitation, from which it is possible to return to the state of Ti^{3+} with octahedral symmetry, in a time of about 0.3 μs, although the contribution of these transitions is about 5 percent. Possibly, coherent interaction of pumping with the crystal increases the probability of these processes and can explain the time delays of development of lasing, experimentally observed in.[5]

In conclusion, we should note that an unambiguous interpretation of the effects described above requires additional unsteady spectroscopic studies and construction of adequate physical and mathematical models of possible mechanisms of relaxation and transfer of energy to impurity crystals upon excitation by high intensity ultrashort pulses.

The authors would like to express their gratitude to G. A. Skripko and N. V. Kondratyuk for providing us with sapphire crystals containing titanium, and also to V. A. Zaporozhchenko for assisting us with the work.

References

1. Moulton, P. E., Opt. News, 1982, Vol 8 No 6, pp 9-15.

2. Nelson, E. D., Wong, I. V., and Shawlow, A. L., Phys. Rev., 1967, Vol 156 No 2, pp 248-305.

3. Kruglik, G. S., Skripko, G. A., Shkadarevich, A. P., et al., Kvant. Electron, 1986, Vol. 13 No 6, pp 1207-1213.

4. Moulton, P. E., J. Opt. Soc. Am. B. 1986, Vol 3 No 1, pp 125- 133.

5. Altshuler, G. B., Karacev, V. B., Kondratyuk, N. V., et al., Pisma v ZhTF, 1987, Vol 13 No 13, pp 779-783.

6. Pestryakov, Ye. V., Petrov, V. V., and Trunov, V. I., V Mezhdunar. Simpoz, "Sverkh bystryye progsessy v spektroskopiy" Tez. dokl. [Fifth International Symposium "Superfast Processes in Spectroscopy" Abstracts of Reports], Vilnyus, 1987, p 76.

7. Sanchez, A., Strauss, Al J., Aggarwal, R. L., et al., IEEE J. Quant. Electr., 1988, Vol 24 No 6, pp 995-1002.

8. Eggleston, J. M., Deshazer, L. G., and Kangas, K. W., IEEE J. Quant. Electr. 1988, Vol 24 No 6, pp 1009-1015.

9. Moncorge, R., Boulton, G., Vivien, D., et al., IEEE J. Quant. Electr. 1988, Vol 24 No 6, pp 1049-1051.

10. Aggarwal, R. L., Sanchez, A., and Stuppi, M. M., IEEE J. Quant. Electr. 1988, Vol 24 No 6, pp 1003-1008.

11. Schmid, F. and Khattak, C. P., Laser Focus, 1983, Vol 19 No 9, pp 147-152.

12. Aleksandrov, A. S., Yelesin, V. F., Lisovets, Yu. P., et al., Kvant. Elektron, 1975, Vol 2 No 2, pp 332-336.

13. Kruglik, G. S., Skripko, G. A., Shkadarevich, A. P., et al., Izv. AN SSSR Cer. Fiz, 1988, Vol 52 No 6, pp 2486-2489.

UDC 621.373.826

Picosecond Optoelectronics

907J0012A Moscow KVANTOVAYA ELEKTRONIKA in Russian Vol 17 No 3, Mar 90 pp 268-287

[Article by P.P. Vasilyev, Institute of Physics imeni P.N. Lebedev, USSR Academy of Sciences, Moscow]

[Abstract] Developments and achievements in the science of picosecond optoelectronics are overviewed, one of the underlying physical principles being generation of an electron-hole pair in a semiconductor upon its absorption of a light quantum and subsequent photoconduction. The speed of this process is limited by the uncertainty relation, it being necessary for the spectrum of an optical pulse to lie within the absorption band which corresponds to transition of electrons from bound to free state and for recombination to subsequently take place sufficiently soon. Interaction of an ultrashort laser pulse and a semiconductor material is another aspect of this fundamental process, inasmuch as this interaction produces a high-density electron-hole plasma in the semiconductor material. Implementation of this physical principle depends on the electrical response of picosecond photoconductors to ultrashort incident laser pulses, the form of the electric response signal being for specifically evaluated for such a device which operates with a microwave microstrip line. Another underlying physical principle, utilized for picosecond strobing, is the linear electrooptic Pockels effect. A review of requirements which sources of optical ultrashort pulses must satisfy is followed by a summary of relevant characteristics of applicable semiconductor materials (α-Si, Si on sapphire, partly disordered Ge, GaP, CdS, CdS_xSe_{1-x}, polycrystalline CdTe, Cr:GaAs, Fe:InP, diamond) and design analysis of electric pulse circuits including transmission lines, optimization of which

requires avoidance of pulse form distortion due to dispersion. Generation of picosecond pulses by semiconductor injection lasers is considered next, including plain modulation of the pump current, Q-switching, and mode locking. A second group of devices are low-voltage, superhigh-speed optoelectronic devices operating by the photoconduction mechanism, correlators of electrical ultrashort pulses, and devices operating on the basis of the electrooptic Vavilov-Cerenkov effect. A third group of devices are laser controlled power switches and shapers of electric picosecond or sub-picosecond pulses, these devices being widely used for experimental research in physics. Four areas of application for optoelectronic devices covered in this report are mentioned here: information processing with the aid of electrooptic gates, measurements with a stroboscopic oscillograph, shaping radio pulses and switching microwave power, and superbroad-band radar. Figures 18; tables 1; references 168.

UDC 621.373.826.038.824

Pulsed Dye Laser With Nonlinear Intracavity Mirror in Photorefractive Crystal

907J0012B Moscow KVANTOVAYA ELEKTRONIKA in Russian Vol 17 No 3, Mar 90 pp 297-299

[Article by S.F. Lyuksyutov and O.I. Yushchuk, Institute of Physics, UkSSR Academy of Science, Kiev]

[Abstract] An experimental pulsed dye laser with a self-recording non- linear intracavity mirror in $LiNbO_3$:Fe photorefractive crystal was built, for the first time so far, the apparatus including a cell with rhodamine 6G solution as active medium in a 30 cm long optical cavity between two plane mirrors with an approximately 0.95 reflection coefficient each and a YAG:Nd^{3+} laser pumping it with second-harmonic radiation tunable over the 550-570 nm range in pulses of 70 mW average power and 20 ns duration at a repetition rate of 10 Hz. The crystal, containing 0.03 wt.% Fe and cut to make its end face perpendicular to its optical C-axis, was placed inside the cavity between the active medium and the front mirror, at a distance from the latter which could be varied over the 1-10 cm range, and its C-axis was slanted relative to the front mirror to ensure adequate amplification of the laser light reflected by the intracavity mirror. A dynamic reflective holographic grating, recorded in the crystal by frequency-degenerate two-beam interaction on a diffuse nonlinearity, served as nonlinear intracavity mirror. The dispersive element, necessary for recording a mirror in the crystal, was either a notched diffraction grating with 600 lines/mm or a prism made of TF-5 or K8 optical glass. A nonlinear intracavity mirror was first recorded using laser radiation within one 100-300 pm wide line and the diffraction grating, no mirror having been obtained without the latter. Covering the front mirror with a shield left only the emission reflected by the intracavity and narrowed the emission line to 10 pm, approximately equal to the spectral selectivity of the holographic grating. The diffraction efficiency of such an intracavity mirror was 0.4-0.5, based on measurement of the relative radiation power reflected by it, with a beam-splitter placed near the crystal surface.The photorefractive crystal was also tested for memory of a multifrequency emission spectrum. The diffraction grating was for this purpose replaced with a glass prism, which made it possible to record a "comb" spectrum, and a Fabry-Perot interferometer with a 1 mm base was inserted into the cavity. The spectrum of multifrequency radiation emitted for 5-10 min was recorded for only 10-100 s, probably owing to an appreciable photogalvanically induced localized response. The authors thank V.Yu. Bazhenov and M.V. Vasnetsov for discussion. Figures 3; references 9.

UDC 621.373.826.038.823

Characteristics of High-Power XeCl-Laser With Electron-Beam Pumping and Their Dependence on Content of Gas Mixture

907J0012C Moscow KVANTOVAYA ELEKTRONIKA in Russian Vol 17 No 3, Mar 90 pp 300-303

[Article by Yu.I. Bychkov, N.G. Ivanov, V.F. Losev, V.V. Ryzhov, I.Yu. Turchanovskiy, and A.G. Yastremskiy, Institute of High-Current Electronics, Siberian Department, USSR Academy of Sciences, Tomsk]

[Abstract] An experimental study of a XeCl-laser with a variable Ar-Xe-HCl active mixture and electron-beam pumping was made for a determination of its power characteristics, depending on the content of that gas mixture and for refinement of its theory. The content of the mixture varied around the Ar:Xe:HCl = 1000:(5-30):(0.5-2.0) range, with a constant pressure of 4 atm. The optical cavity was formed by an aluminum mirror and a plane-parallel quartz plate. An electron beam from a pulsed vacuum diode-gun was injected into the laser chamber from two opposite sides through two windows made of 50 μm thick titanium foil and spaced 13 cm apart. The power of laser emission was measured on the symmetry axis of laser chamber at a distance of 2 cm from one of the windows. The maximum power density of 0.75 MW/cm^3 and maximum duration of a laser pulse were attained with an Ar:Xe:HCl = 1000:10:1 mixture under a total pressure of 4 atm. Increasing the HCl concentration lowered the emission power and lengthened the time lag of an emission pulse behind a pump pulse. The results of this experiment are supplemented with a theoretical model of the plasmochemical reactions and their kinetics in such an active medium. Construction of this model requires first calculating the distribution of absorbed pump power over the active volume, as a function of time, which has been done by the Monte Carlo method, considering the current density on a window foil at successive instants of time and assuming, for simplicity, a monoenergetic electron beam from a

point source. In the analysis, in addition to the plasmochemical reactions, those also included were processes of superelastic impact HCl(v = 2)+ e → HCl(v = 0)+ e and HCl(v = 1)+ e → HCl(v = 0) + e, cascade excitation HCl(v = 1)+ e → HCl(v = 2)+ e, and de-excitation of vibrational levels HCl(v = 2)+ e → HCl(v = 1)+ e. The pump mu-power density has been calculated, on the basis of such a simulation, as a function of both time and distance between window foils. Other factors taken into account are the following parameters as functions of time: coefficients of radiation absorption by $ArXe^+$, Cl^-, and XeCl molecules, concentrations of HCl in states v = 0,1,2, con- centration of electrons, and concentrations of XeCl in states C,B,X. Both delay and the duration of an emission pulse is found to depend largely on the concentrations of HCl and Xe in the active mixture. Figures 6; references 10.

UDC 681.4

Optimum-in-Speed Algorithms for Adaptive Optical Systems With Flexible Mirrors

907J0012D Moscow KVANTOVAYA ELEKTRONIKA in Russian Vol 17 No 3, Mar 90 pp 370-373

[Article by D.A. Bezuglov, Rostov Higher Command-Engineering School for Missile Armed Forces, Rostov-na-Donu]

[Abstract] Design optimization of adaptive optical systems with flexible mirrors for high speed aperture scanning with multichannel phase modulation in a turbulent atmosphere is considered, a major difficulty not encountered in the design of other adaptive systems being the $2\pi n$-problem of local maxima and stationary points. Three different algorithms of adaptive control are constructed to ensure fast convergence of the performance criterion to its maximum value without loss of stability. Radiation is assumed to propagate from a point source through a turbulent atmosphere which distorts its phase front and to arrive, together with a white Gaussian random background noise, at the receiver aperture in homogeneous medium, the receiver being a flexible mirror with N drives which corrects the phase front and then reflects the radiation into a quasi-point small photodetector in the focus of a converging lens. The mirror profile and the perturbation of its surface are described in terms of a set of j = 1,...,N functions S_j of the radial coordinate which characterize the influence of each of the N drives, assuming a linear response of the mirror to control actions. Inasmuch as the radiation intensity on the photodetector cannot be expressed in an analytical form, a linear transformation of the control coordinates replaces the influence functions with elements of the inverse of the mirror compliance matrix. All three algorithms were tested on a computer for speed of convergence for a rectangular mirror, depending on the number of mirror drives N and on the signal-to-noise ratio, with the radiation intensity at the center of the photodetector as performance criterion and a generator of random numbers with a normal distribution, simulating a turbulent atmospheric channel. Only the third algorithm for the calculation of weight coefficients of matrix elements (influence functions) $b_{im+1} = B_{im}G^{-1N-1}gradJ(B_{im)+n_m}$ (n_m-noise in channels on m-th step) does not require inversion of a matrix of second derivatives on each step and allows complete elimination of cross-couplings in the control channel. Not all N^2 elements of the G^{-1} matrix need to be stored in the computer memory, only two weight coefficients should be stored. The second algorithm allows elimination of cross-couplings on the mirror only, and the first algorithm tends to become unstable when the signal-to-noise ratio in the control channel is low. Figures 3; references 6.

Absorption of Laser Radiation by Spherical Shell Microtargets and Their Degree of Compression in Bursting Mode

907J0014A Moscow ZHURNAL EKSPERIMENTALNOY I TEORETICHESKOY FIZIKI in Russian Vol 97 No 3, Mar 90 pp 834-841

[Article by S.A. Belkov, A.V. Bessarab, A.V. Veselov, S.G. Garanin, G.V. Dogoleva, A.I. Zaretskiy, G.A. Kirillov, G.G. Kochemasov, N.V. Maslov, I.N. Nikitin, S.I. Petrov, A.V. Ryadov, A.V. Senik, N.A. Suslov, and S.A. Sukharev]

[Abstract] An experimental study was made involving irradiation of spherical glass microtargets with radii of 120-240 μm by an "Iskra-4" iodide laser at the 1.315 μm wavelength, with an intensity of 10^{14}-10^{15} W/cm^2 in pulses of 0.2-0.4 ns duration. The aspect ratio $R_0/\Delta R$ of the glass shells varied around the 30-120 range. The first experiment yielded data on absorption of laser radiation by the plasma corona as well as by the target body, measurements having been made with pyroelectric detectors as calorimeters, also on the generation of fast particles along with the emission of hard x-rays. The dependence of the absorption coefficient, the energy of fast ion, the temperature of hot electrons, and the energy of x-rays on the intensity and the angular dis-tribution of incident laser radiation has revealed a definite role of reso- nance absorption. The second experiment, with laser pulses of 300-400 J energy and 0.2-0.35 ns duration, has yielded data on bulk compression and on the finite density of generated deuterium-tritium gas. Determinations had been made based on the size of the image of a target core projected by intrinsic x-rays in a camera obscura with high space resolution but no time resolution, based on the size of the space lit by Ne-line glow upon addition of neon to the DT gas so that its partial pressure did not exceed 7% of the total, and based on the spectral width of both Ly(β) and Ly_γ Ne X lines in the Lyman series of hydrogen-like neon. In this experiment, the line spectrum of x-rays was recorded in a KAP-crystal spectrograph with space resolution, and the microshells were coated with a 0.5-3 μm thick film of the C_8H_8 plastic. The results of numerical calculations for the one-dimensional model of gas dynamics agree on a relative basis but not on a quantitative (absolute value)

basis according to the results of these two experiments. Figures 6; tables 1; references 16.

Collective Pinning of Soliton Array in Josephson Junctions

907J0014D Moscow ZHURNAL EKSPERIMENTALNOY I TEORETICHESKOY FIZIKI in Russian Vol 97 No 3, Mar 90 pp 976-988

[Article by V.M. Vinokur and A.Ye. Koshelev, Institute of Solid-State Physics, USSR Academy of Sciences]

[Abstract] Both field and temperature dependence of the critical current on nonhomogeneous long Josephson junctions is analyzed. An earlier study has revealed that ceramics with a small coherence length and a high superconducting transition temperature, the trend of this dependence is determined essentially by thermal fluctuations of the vortex structure. A planar nonuniformly distributed Josephson junction is considered, its energy being expressed in the form of a double integral in the three terms which represent - energy proportional to the mean density of the critical current in absence of a magnetic field, the random potential associated with spatial fluctuations of that density, and energy proportional to the density of the actual current flowing through the junction, each term with a correction factor accounting for the phase difference between the junction. The critical current at T = 0 temperature is estimated on the basis of dimensional and correlational analyses, for a junction with collective pinning of an Abrikosov vortex array, or a junction with dimensions larger than the the correlation length, or in a point junction. As the magnetic field intensity is raised beyond the lower critical, the critical current for all three kinds of junction is found to drop to a plateau and to cease being field-dependent. Both temperature and field dependence of the critical current is estimated on the basis of the current-voltage characteristic, particularly its trend in the high-current range, by expansion in the random potential. It is taken into consideration that at any temperature above zero there corresponds a finite voltage, across a junction with a finite area, to an arbitrary small current, the critical current being the current at which the the resistance of the junction becomes normal. This critical current is found to depend similarly on the ratio $\delta_J \lambda H/\Phi_0$ (H-magnetic field intensity, δ_J-Josephson penetration depth, λ-London penetration depth, Φ_0-flux quantum) for one-dimensional and two-dimensional junctions, being consistently lower for a one-dimensional junction but dropping to the same plateau as the critical value of this ratio is exceeded. The effect of thermal fluctuations in a soliton array on the critical current for a two-dimensional junction is estimated. This is done by including the Debye-Baller factor and thus decreasing the correction for the critical current to an exponential multiplier. They are not found to influence the magnitude of the critical current for a two-dimensional junction but to lower it appreciably for a sufficiently thin one-dimensional one. The temperature dependence of the minimum critical current is, according to the estimates based on dimensional analysis, $j_{c,min}$ varies as $(T_c\text{-}T)^{3/2}$ for a two-dimensional SIS junction and as $(T_c\text{-}T)^{7/9}$ for a two-dimensional SNS junction. The effect of the intrinsic magnetic field on the junction current is also estimated, its effect being essentially a nonuniform distribution of the resultant magnetic induction and consequent constraints. These constraints are much more severe for a two-dimensional junction than for a one-dimensional one. Figures 2; references 18.

UDC 621.378.325

Emission of Picosecond Pulses by Holographic Dye Laser With Distributed Feedback and Nanosecond Excitation

907J0029A Minsk ZHURNAL PRIKLADNOY SPEKTROSKOPII in Russian Vol 52 No 2, Feb 90 pp 202-206

[Article by V.Yu. Kurstak, A.N. Rubinov, S.A. Ryzhechkin, and T.Sh. Efendiyev, Institute of Physics, BSSR Academy of Sciences, Minsk]

[Abstract] An experimental study has established the feasibility of stable emission of separate picosecond pulses which have a bounded spectrum by a dye laser with distributed feedback, excited by nanosecond radiation pulses from a nitrogen laser. The active medium of the dye laser was an ethanol solution of coumarin-1 poured into, but not pumped through, the cell. An industrial LGI-505 nitrogen laser served as source of excitation emitting pulses of 10 ns duration with a peak power of 25 kW, their repetition rate being varied up to 1 kHz. The time characteristics of emission were measured in an "Agat-SF3" electron-optical camera with 1.9 ps resolution. The spectral width of the emitted 485.6 nm radiation was measured with a Fabry-Perot interferometer, while the pulse energy was measured with the aid of FD-24K photodiodes and an S8-13 oscillograph. The duration of the first single picosecond emission pulse decreased from 80 ps to 35 ps as the excitation energy was increased from the threshold to 1.5 times the threshold and did not decrease further. The pulse duration, the threshold excitation power density, the pulse energy, were all found to depend on the length of the feedback structure and on the dye concentration. The pulse duration decreased linearly from 67 ps to 46 ps and the pulse energy decreased linearly from 32 nJ to 17 nJ as the dye concentration was increased from 0.005 mol.% to 0.02 mol.%, while the threshold excitation power density decreased nonlinearly. As the length of the feedback structure was increased from 2 mm to 7 mm, the pulse energy increased linearly from 15 nJ to 42 nJ. The spectral width of 80 ps pulses and 55 ps pulses was 0.0015 nm and 0.003 nm respectively, the ratio of pulse width to spectral width remaining constant even for a single pulse and depending only on the excitation energy above threshold level. In order to facilitate emission of

pulses at repetition rates of 800-1000 Hz, it was necessary to readjust the nitrogen laser for a different distribution of radiation intensity over the cross-section of the pumping beam. Figures 4; references 5.

Outlook for Laser Pumping of Atomic Frequency Discriminators

907J0037A Leningrad ZHURNAL TEKHNICHESKOY FIZIKI in Russian Vol 60 No 3, Mar 90 pp 162-166

[Article by Ye.B. Aleksandrov]

[Abstract] Changeover from optical gas-discharge pumping to laser pumping of atomic frequency discriminators, operating as frequency standards is considered. This would broaden the range of devices using them, the principal advantage of a laser being its monochromaticity in the sense of its narrowness of single spectral line rather than of its mere existence. Atomic frequency discriminators using two-level atoms are, from this standpoint, comparatively evaluated for sensitivity with gas-lamp pumping and with laser pumping respectively. Their sensitivity is defined as the ratio of derivative $dI/d\Delta$ to $I^{1/2}$ (I-intensity of pumping radiation, Δ-deviation from 1-2 transition frequency, $I^{1/2}$-quantity proportional to shot noise intensity in the photodetector). The theoretical analysis leading to this evaluation is based on the Voigt profile describing both emission and absorption cross-sections of such a device, with reabsorption simulated by additional self-absorption. The result obtained is the dependence of the discriminator sensitivity on the relative pumping rate, corresponding to various initial optical densities of the active medium and on the relative pumping intensity in two different pumping modes characterized by parameter $\kappa = 0$ or 1.5 respectively. The maximum sensitivity at some pumping rate or at some pumping intensity is not more than twice as high with laser pumping and requires only one-half to one-third the intensity then, but is less sensitive to variations of the spectral contour in the case of optical gas-discharge pumping. Figures 3; references 9.

Experimental Study Relating to Angular Characteristics of Relativistic High-Power Electron Beam of Microsecond Duration

907J0037B Leningrad ZHURNAL TEKHNICHESKOY FIZIKI in Russian Vol 60 No 3, Mar 90 pp 172-180

[Article by S.G. Voropayev, B.A. Knyazev, V.S. Koydan, S.V. Lebedev, V.V. Chikunov, and M.A. Shcheglov, Institute of Nuclear Physics, Siberian Department, USSR Academy of Sciences, Novosibirsk]

[Abstract] An experimental study of a relativistic electron beam with high current density and of microsecond duration, eminently suitable for heating of a plasma inside a solenoid was made; its object being the angular characteristics of such an electron beam. The beam with a diameter of 20 cm was generated in a vacuum diode having a graphite cathode and a 10 μm thick aluminum-coated dacron foil or a 30 μm thick or 90 μm thick aluminum foil on dacron as anode, under a voltage of 0.9 MV maximum and in a longitudinal magnetic field of 5 kG intensity. With a current density of 0.3 kA/cm^2, the beam current reached 50 kA and the beam energy at the exit from the diode reached 130 kJ. Upon passage through a thin foil acting as the anode, the beam entered a drift chamber where it was adiabatically compressed over a 25 cm long first segment to a 20 times smaller cross-section in a magnetic field climbing to 100 kG intensity and then expanded to its original cross-section over the next channel segment. The experiment was performed in the U-1 accelerator facility, the divergence of this electron beam immediately behind the anode and upon leaving the compression zone, measured by two methods. First, it was determined on the basis of the current drop during passage of the paraxial core of the beam through a segmented cylindrical small-diameter channel, with a special divergence-angle transducer situated on the axis of a beam collector made of graphite with a center hole comparable in size with the Larmor radius of the electron beam. Then, with a 10 μm thick second foil made of aluminum-coated dacron behind the magnetic plug, it was estimated on the basis of changes in the reflection coefficient. An accuracy analysis of both methods considering the dependence of the absorption coefficient on the channel length and on the divergence angle, is followed by an evaluation of the experimental data which include voltage and current oscillograms as well as divergence-angle oscillograms, which are recorded behind the anode with and without subsequent compression (with and without the second foil) as well as behind the compression zone. Accordingly, the beam divergence angle was 5.8+/1.7° behind the anode without subsequent compression and 26+/-8° in the magnetic plug. Under low pressure in the compression segment within the 10^{-3}-10^{-4} Pa range, it was found to be possible to appreciably decrease the beam divergence angle. The authors thank D.D. Ryutov for interest and helpful discussions. Figures 6; references 18.

Electrical Resistance of Medium With Fractal Structure

907J0002C Moscow ZHURNAL EKSPERIMENTALNOY I TEORETICHESKOY FIZIKI in Russian Vol 97 No 1, Jan 90 pp 373-382

[Article by V.F. Gantmakher, S.E. Yesipov, and V.M. Teplinskiy, Institute of Solid-State Physics, USSR Academy of Sciences]

[Abstracts] Transition of the 40Zn-60Sb alloy from the metastable crystalline metallic phase to the amorphous dielectric phase is analyzed, theoretically with the aid of experimental data on the temperature dependence of its electrical resistance at successive stages of that transition, its electrical resistance $R(T,d) = R_1(T,d) + R_0(d)$ depending not only on the temperature T but also on a microgeometrical dimension d which characterizes the degree of amorphization. The character of the material and its geometry are each identified by expressing the electrical resistance as a product of electrical resistivity and a macrogeometrical form factor Φ, this form factor being a function of the microgeometrical dimension d and namely inversely proportional to the latter cubed. This conclusion has been reached on the assumption that the amorphous phase with a negligible electrical conductivity insulates crystalline metallic conduction channels, these channels existing until the transition is complete and their effective width d reduced to zero. Taken into consideration is the classical size effect in the conduction channels, attributable here to scattering of charge carriers by their metallic walls. Growth of the amorphous phase is viewed from the standpoint of amorphization kinematics and, accordingly, moving knife-edge amorphization front subject to three rules: (1)such a front is turned around by weak plane boundaries of inelastic regions, (2)its thickness increases very slowly owing to the compressed state of the surrounding medium, and (3)it comes to a standstill upon an encounter with another such front. The characteristic dimensions of the amorphous component and the form factor of the conduction channels are then described in terms of generations of an evolving fractal structure. As a model of a conduction channel is subsequently considered the diffusion trajectory of a Brownian particle, with dimensionality 2 in a 3-dimensional space and with loops self-intersecting on it. Deviation from the universal temperature dependence of the electrical resistance is then attributed not only to the amorphous phase, whose thermally activated electrical conductivity, rather than the weak tunneling, increases with rising temperature, but also to the attendant shunting of nonintersecting loops along diffusion trajectories. The authors thank V.V. Tvardovskiy and D.Ye. Khmelnitskiy for helpful discussions, O.I. Barkalov, I.T. Belash, and Ye.G. Ponyatovskiy for interest. Figures 5; references 8.

Scattering of Neutrinos by Nuclei in Matter

907J0007A Moscow PISMA V ZHURNAL EKSPERIMENTALNOY I TEORETICHESKOY FIZIKI in Russian Vol 51 No 5, 10 Mar 90 pp 237-238

[Article by L.B. Leinson, Institute of Terrestrial Magnetism, Ionosphere, and Radio Wave Propagation]

[Abstract] Inasmuch as the interaction of nuclei in a dense collapsing matter when the latter is impermeable to neutrinos, reduces the spectrum of low-momentum excitations in it to an acoustic one, the scattering of neutrinos by its nuclei should amount to emission and absorption of photons. The cross-section for scattering by an isolated nucleus is, therefore, not the same when calculated for the central part of a collapsing star as when calculated for an ideal gas of spinless nuclei. The interaction of neutrinos with nuclear density fluctuations is, accordingly, described by a Hamiltonian which includes coherent interaction of a neutrino with all nucleons of a nucleus through neutral currents. When the energy of the sound wave is much smaller than that of the neutrinos, then their scattering becomes elastic and the cross-section for scattering them is obtained by integrating its differential with respect to the cosine of the scattering angle referred to one nucleus. Scattering of neutrinos by nuclei of a medium at zero absolute temperature amounts to spontaneous emission of photons. At a temperature much higher than the product Ec (E-energy of neutrino, c-speed of sound) stimulated emission and absorption of photons is predominant. references 5.

New Kondo Lattice in $CeSi_{2-x}Ga_x$ System

907J0007B Moscow PISMA V ZHURNAL EKSPERIMENTALNOY I TEORETICHESKOY FIZIKI in Russian Vol 51 No 5, 10 Mar 90 pp 286-289

[Article by V.V. Moshchalkov, O.V. Petrenko, M.K. Zalyalyutdinov, and I. Chirich. Moscow State University imeni M.V. Lomonosov]

[Abstract] A new nonmagnetic Kondo lattice with a giant Abrikosov-Suhl resonance was sought and found in the $CeSi_{2-x}Ga_x$ heavy-fermion superconducting system. Its existence in polycrystalline specimens within the single-phase range of Ga concentration x = 0.7-1.3 has been established on the basis of specific heat and electrical resistivity measurements over the T = 4.2-300 K temperature range. The temperature dependence of c/T based on c(T) measurements agrees roughly with the temperature dependence of c/T based on the Cockblin-Schrieffer model of specific heat and the Wiegmann-Andrew method of its calculation. The dependence of the coefficient γ characterizing its electronic component γT on the exchange interaction integral J is characterized by a sharply rising peak about the critical value of that integral. The entropy associated with this low-temperature anomaly has been estimated from the area under the C/T(T) curve, the increment of entropy ΔS being approximately 4.69 J/K or $R\log_e 2$ for all materials in this system with x within the given range. This indicates that the magnetic level j = 5/2 of Ce^{3+} ions is widely split by the crystal field, the lowest state being a doublet and the location of the two levels corresponding to two characteristic Kondo temperatures: T_{high} (119 K for x = 1.2-1.3) and T_{low} (19 K for x = 1.2-1.3). The magnetic component of the electrical resistivity was found to be maximum at a temperature about 100 K, its

temperature dependence over range having been calculated by subtracting the electrical resistivity of $LaSi_{2-x}Ga_x$ from that of $CeSi_{2-x}Ga_x$ for each x and the temperature corresponding to that maximum found to shift slightly upward with increasing Ga content. Figures 3. references 8.

Soliton Model of Elementary Electric Charge

907J0009A Moscow TEORETICHESKAYA I MATEMATICHESKAYA FIZIKA in Russian Vol 82 No 3, Mar 90 pp 349-359

[Article by A.P. Kobushkin and N.M. Chepilko, Institute of Theoretical Physics, UkSSR Academy of Sciences]

[Abstract] Existence of three-dimensional topologically stable solitons is shown to be possible, based on the electrodynamics of a scalar Klein-Gordon field according to its nonlinear theory, whereupon these solitons are shown to be available as a model of an elementary electric charge without the divergence of momentum integrals found in Landau-Lifshits models. Following an interpretation of nonlinear Klein-Gordon one-particle field electrodynamics in terms of a distributed electric charge on a Minkowski manifold, which leads to the chiral model of electromagnetism at the zero Planck constant limit, the virial theorem is applied to prove the topological stability of such solitons. The centrisymmetric electrostatic unperturbed solution to the system of field equations does, accordingly, describe an elementary electric charge with zero spin and a rotating electrostatic soliton. Then it describes one with a spin, a magnetic moment being quantizable at the center and characterizing a magnetic dipole at the periphery of such a soliton. The authors thank G.M. Zinovyev and participants of the seminar held by the Department of High Energy-Density Physics for helpful discussions, and M.I. Derkach for performing the numerical calculations. Figures 2; references 9.

Interpretation of KAMIOKANDE Neutrino Experiment

907J0010B Moscow YADERNAYA FIZIKA in Russian Vol 51 No 3, Mar 90 pp 774-776

[Article by E.V. Bugayev, Institute of Nuclear Research, USSR Academy of Sciences, Moscow, and V.A. Naumov, Irkutsk State University]

[Abstract] For an interpretation of data on the low-energy atmospheric neutrino flux recorded by the neutrino detector in recent KAMIOKANDE-I,II experiments, four kinds of neutrino events characterizing this flux were counted on the basis of the authors' earlier calculated neutrino spectrum and with corrections for polarization of muons produced in $\pi_{\mu 2}$ and $K_{\mu 2}$ decays. The calculated total number of neutrino events $N_{SR}+N_{MR}$ as well as numbers of single-ring events $N_{SR} = N_M+N_S$ and of multiring events N_{MR} agree closely, each with the corresponding number recorded, while the calculated number of electron-like single-ring events N_S and number of muon-like single-ring events N_M are respectively 19% lower and 20% higher than the corresponding numbers recorded. The calculated ratio N_S/N_M, moreover, is 48% lower than that based on the experimental data. These differences exceed the estimated 10% calculation error and must be explained otherwise. Most probable seem to be either two-neutrino ν_e—$_\mu$ oscillations or three-neutrino oscillations with the $\nu_\mu \rightarrow \nu_e$ transition in a dominant role. Misidentification of events in the experiment is, moreover, highly probable because of the following: inadequate detector precision for pinpointing the vertex of a single-ring event, the small difference between the angles of multiple muon scattering and multiple shower electron scattering near the recording threshold, an ubiquitous diffuse light emitted by δ-electrons along the tracks of non-shower muons, and inelastic νN-reactions with absorption of pions by ^{16} O nuclei and subsequent emission of γ-quanta capable of generating electron-positron pairs whose appearance then simulates an electronic-like single-ring event. The authors thank S.P. Mikheyev for helpful discussions. Tables 1; references 19.

UDC 539.2

Breaking Solitons, Part 3

907J0011A Moscow IZVESTIYA AKADEMII NAUK SSSR: SERIYA MATEMATICHESKAYA in Russian Vol 54 No 1, Jan 90 pp 123-131

[Article by O.I. Bogoyavlenskiy]

[Abstract] Considering that the two-dimensional nonlinear equation $u_{tx} = 4u_xu_{xy}+2u_yu_{xx}-u_{xxxy}$ where $u_t = \delta(\text{partdiff})^{X-1}\ \delta(\text{var})H/\delta(\text{var})u$ reduces to the Korteweg-deVries equation with a corresponding Hamiltonian when y is identically equal to x and both equations have an exact solution, and a breaking soliton, both Gardner and Miura transformations are applied to that two-dimensional modification and, with the aid of a special theorem, this equation is shown to also have an innumerable set of first integrals representing conservation laws. This equation is then reformulated in the Lax representation, following a factorization of the Schroedinger operator, whereupon integral complex versions of both equations are constructed and periodic, as well as breaking solutions, are analyzed. References 9.

"Supersolitons" in Periodically Nonhomogeneous Long Josephson Junctions

907J0014C Moscow ZHURNAL EKSPERIMENTALNOY I TEORETICHESKOY FIZIKI in Russian Vol 97 No 3, Mar 90 pp 924-937

[Article by B.A. Malomed, Institute of Oceanology, V.A. Oboznov and A.V. Ustinov, Institute of Solid-State Physics, USSR Academy of Sciences, Moscow]

[Abstract] The behavior of periodic fluxon chains in a long Josephson junction containing a periodic array of artificial inhomogeneities is analyzed. Taken into consideration, the effective density of the lateral current which breaks a fluxon chain pinned to such an array, the density of the chain and thus proportional to its magnetic field intensity at the edges of the junction. This dependence is characterized by narrow peaks about points corresponding to commensurate fluxon chain and periodic array, but deformation waves can still propagate along a pinned fluxon chain even at a current density below critical, owing to the finite rigidity such a chain. This is the case when the fluxon chain is almost commensurate with the periodic array, either having one extra fluxon or missing one and such a defect being shifted along the chain. Analysis of this phenomenon is based on the theoretical model of superconduction electrons in a nonhomogeneous long junction. The evolution of a local phase difference in their wave equation is described by the sine-Gordon equation, corresponding to which the total Hamiltonian of this model is the sum of three Hamiltonians representing the quiescent system, the chain-array interaction, and the lateral current respectively. Assuming a deformation scale much larger than the array period, the total Hamiltonian generates an elliptic sine-Gordon equation which describes one supersoliton or two colliding ones. A numerical solution of this equation by the method of finite differences according to a stabilized explicit scheme has yielded the current-voltage characteristics of such a junction containing either equal or unequal numbers of inhomogeneities and fluxons. An experiment was performed with distributed $Nb/NbO_x/Pb$ junctions produced according to standard technology: magnetron sputtering of niobium, photolithography, niobium oxidation by plasma treatment, lead deposition by heat treatment. Periodic spatial modulation of the critical current density was attained by deposition of SiO strips on the Nb film surface prior to the oxidation process so as to build in a periodic array of transverse inhomogeneities for spatial modulation of the critical current density. These strips, uniformly spaced along a 20 μm wide junction, were 150 nm thick and 12 μ wide. With nine such strips in a 498 μm long junction, the modulation period was approximately 50 μm and the Josephson penetration depth at 4.2 K temperature was approximately 30 μm. Measurements were made at that temperature in a magnetic field whose intensity was varied up to 4 Oe. They revealed two series of anomalous voltage-step singularities on the current voltage characteristics, the first series * appearing at magnetic field intensities higher than H_1 (1.49 Oe) but lower than H_2 (3.01 Oe and the second series ** appearing at magnetic field intensities higher than H_2. The maximum magnitude of these voltage steps was found to depend on the magnetic field intensity. The authors thank I.V. Vernik, V.M. Vinokur, A.A. Golubov, V.E. Zakharov, V.P. Koshelts, N.Ye. Kulagin, K.K. Likharev, V.V. Ryazan, V.K. Semenov, D.Ye. Khmelnitskiy, and I.F. Shchegolev for discussion, N.S. Stepakov for assisting in preparation of the experiment. Figures 8; references 19.

New Confinement-Deconfinement Order Parameter in Lattice Theories

907J0022A Moscow PISMA V ZHURNAL EKSPERIMENTALNOY I TEORETICHESKOY FIZIKI in Russian Vol 51 No 6, 25 Mar 90 pp 296-297

[Article by U.-E. Wiese and M.I. Polikarpov, Institute of Theoretical and Experimental Physics]

[Abstract] A new order parameter is proposed pertaining to the mechanism of confinement in accordance with the model of a vacuum which contains a superconducting condensate of magnetic monopoles. Numerical calculations were made based on the theory of four-dimensional compact lattice electrodynamics, considering that gauge fields in this theory are defined in modulo-2π terms so that monopoles do exist here. The results of these calculations indicate that a dual lattice in the confinement phase is densely covered by current lines with many self-intersections, the current lines being closed ones by virtue of the conservation law. The fractal dimensionality d, moreover, is nontrivial in the confinement phase ($\beta < \beta_c$) and $d = 1$ in the deconfinement phase ($\beta > \beta_c$). The proposed parameter, therefore, corresponds qualitatively to a condensate of magnetic monopoles in the confinement phase with a magnetic current density so high as to make the dimensionality of clusters higher than 1. In the deconfinement phase, meanwhile, the dimensionality of clusters formed by magnetic currents is $d = 1$ at temperature above critical and $d > 1$ at temperatures below critical. The fractal dimensionality of lines is now defined as the ratio of the number of lattice edges occupied by a current line to the number of lattice nodes through which a current line passes. The authors thank A. DiGiacomo for helpful discussions. Figures 1; references 8.

Diamagnetic Soliton on Twin Boundary

907J0022B Moscow PISMA V ZHURNAL EKSPERIMENTALNOY I TEORETICHESKOY FIZIKI in Russian Vol 51 No 6, 25 Mar 90 pp 310-314

[Article by S.N. Burmistrov and L.B. Dubovskiy, Institute of Atomic Energy imeni I.V. Kurchatov]

[Abstract] The occurrence of diamagnetism at the bicrystal boundary is analyzed, an anomalous magnetic susceptibility at such boundaries in simple metals having been revealed by measurements of the Knight shift and muon spin relaxation not only at low temperatures but also at all normal ones. A functional relation between the magnetic induction B and the magnetization current j in a symmetric bicrystal, namely a twin crystal, is established on the basis of Maxwell equations which, for this case, reduce to $-dB/dx = 4\pi/cj$ (vector B in z-axis, vector j on z-axis, both vectors in twinning plane perpendicular to x-axis). While the magnetization in the vicinity of the twinning plane is found to be always nonuniform in space with an external magnetic field present, the necessary and sufficient condition for spontaneous magnetization in this vicinity to occur in the absence of an

external magnetic field is found to be that j become proportional to B^{α} ($0 = or < \alpha < or = 2$) as $B \rightarrow 0$. An oblique twinning boundary layer, much thinner than the radius of an electron orbit, is considered in an anisotropic metal and its behavior in a magnetic field, equivalent to that of a potential barrier, is described by the appropriate Hamiltonian. Owing to the symmetry of a twin crystal with respect to the twinning boundary, the same external magnetic field induces in equal but opposing currents in the two halves so that the magnetizing current is an odd function of the x-coordinate: $j(-x) = -j(x)$. Estimates of $j(x)$ for $\alpha = 0$ indicate the possibility of a soliton of amplitude B forming on the twinning boundary with a magnetic field symmetric with respect to that boundary. The form of this soliton is found by simultaneously solving the Maxwell field equation and the material equation which relates $j(x)$ to $B(x)$, this system of equations being most simply closed by a local approximation for $B(x)$. Such a closure, though not entirely self-consistent, is adequate when the characteristic scale of $B(x)$ variation is much larger than the radius of an electron orbit. The authors thank the Science Council on high-temperature superconductors for support in carrying out project No 174 of the government-sponsored "High-Temperature Superconductivity" program. Figures 2; references 7.

Fractal Vibrational Excitations in Polymers

907J0022C Moscow PISMA V ZHURNAL EKSPERIMENTALNOY I TEORETICHESKOY FIZIKI in Russian Vol 51 No 6, 25 Mar 90 pp 314-317

[Article by M.G. Zemlyanov, V.K. Malinovskiy, V.N. Novikov, P.P. Parshin, and A.P. Sokolov, Institute of Automation and Electrometry, Siberian Department, USSR Academy of Sciences]

[Abstract] An experimental study of fractal vibrational excitations in a disordered polymer material was made, polymethyl methacrylate being such a material. The density of vibrational states in film specimens of this material was obtained by measurements of inelastic neutron scattering and from this data then was determined the spectral dimensionality d of fractons in PMMA film specimens. Data on the fractal dimensionality D was obtained by Raman light-scattering spectroscopy. Both sets of data were combined for a determination of the "superlocalization" parameter d_{φ} and then, combined together with the other two parameters of the fracton wave function. The neutron scattering spectrum was measured by by the time-of-flight method at 30°, 45°, 75°, and 90° scattering angles, the "generalized" vibration spectrum having then been calculated in the noncoherent approximation directly without use of any models. Interpretation of the data on Raman scattering of light by fractons requires a special inelastic scattering theory, such a theory is proposed which treats interaction of light and fractons as a continuous process. Matrix element M_i of interaction with a fracton localized at a point r_i is, according to this theory, determined by the gradient of the wave function on that fracton. With the aid of Fermi's golden rule and with the Raman scattering intensity normalized to the Bose factor, considering that the fractal dimensionality for polymers is approximately D = 2, an evaluation of the experimental data according to this theory yields $d_{\varphi} = 1.5$ and 2.5 for noncoherent vibrational excitations and for coherent ones respectively. The author thanks V.A. Bagranskiy for supplying the PMMA specimens. Figures 2; references 13.

UDC 537.874.6

Method of Constructing New Forms of Solutions to External Problems of Electrodynamics for Intricately Shaped Regions

907J0026A Moscow DOKLADY AKADEMII NAUK SSSR in Russian Vol 311 No 1, Mar 90 pp 67-71

[Article by V.F. Kravchenko, Academician V.L. Rvachev, UkSSR Academy of Sciences, and T.I. Sheyko]

[Abstract] New forms of solutions to external problems of microwave electrodynamics for intricately shaped regions are shown, the method of constructing these solutions being based on the theory of R-functions. This method, an analytical one which makes full use of a priori information about the sought solution and which facilitates numerical solution for intricately shaped regions with the aid of "FIELD" system program generator, is demonstrated on the two-dimensional Dirichlet problem for the scalar theory of diffraction. Let the boundary $\delta\Omega$ of region Ω be a C^2-manifold describable by the equation $\omega(x)$ in C^2, (x in R^n-space. If it is a boundary with C^0 smoothness, its nondifferentiable segments can be "smoothened" by special R-operations so that the region becomes transformed into one with a boundary of necessary smoothness and yet differing, sufficiently little, from the original one. The solution is constructed in two steps; in the first step is constructed a function $\omega(x,y)$ defined everywhere with the given region and satisfying the boundary conditions at that region's boundary as well as the Sommerfeld condition at infinity. The second steps involves constructing, by any one of variational procedures, coordinate sequences of complete and linearly independent functions which will satisfy the original Helmholtz wave equation. Figures 2; references 14.

UDC 539+621.039

Multiple Scattering of Charged Particle in Bent Crystals

907J0026B Moscow DOKLADY AKADEMII NAUK SSSR in Russian Vol 311 No 1, Mar 90 pp 72-74

[Article by V.A. Muralev and N.I. Kozlov, Institute of Applied Mathematics imeni M.V. Keldysh, USSR Academy of Sciences, Moscow]

[Abstract] Use of crystals for controlling beams of charged particles is considered, bent crystals having

already been used in experiments (Dubna, CERN, Batavia-USA laboratories) for deflection and attenuation of proton beams. A theoretical analysis of the process is based on description of target flexure along a planar path in terms of centrifugal action, the resulting asymmetry of the transverse planar potential knocking the equilibrium orbit of particles out of the region of minimum potential in an originally straight target. The potentials of bent planar channels are described by the approximating expression Y(X) = U(X)+PVX/R-min[U(X)+PVX/R], where U(X) denotes the planar potential, P denotes the particle momentum, V denotes the particle velocity, and R denotes the radius of target curvature. This model is used as a basis for refining the geometry of real crystal targets, considering that such a target consists of a straight region which faces the incident beam and a bent region where particles are scattered. The equations of kinetics, which yield the distribution of bound and suprabarrier particles in the region where the radius of curvature varies, reduced to two-dimensional ones which take into account loss of particle energy due to scattering and the kinetic coefficients here depend additionally on the depth of particle penetration. The momentum P (GeV/s) and P/R (GeV/s.m) distribution of the fraction of protons χ(P/R) deflected by the region of a silicon crystal bent in the (111) direction and the dependence of the deflection length $\chi_{0.5}$(M) for protons on the energy contained in that bent region have been evaluated on the basis of this theoretical model and also on the basis of experimental data from Batavia. Discrepancies have been reconciled to the extent that both theory and design of target bending for proton beam control can be further refined. Article was presented by Academician Ye.P. Velikhov on 24 Feb 89. The authors thank Professor M.A. Kumakhov for discussion of pertinent problems. Figures 2; references 4.

Propagation of Periodic Ultrashort Pulses Through Nonlinear Optical Fibers

907J0002A Moscow ZHURNAL EKSPERIMENTALNOY I TEORETICHESKOY FIZIKI in Russian Vol 97 No 1, Jan 90 pp 144-153

[Article by A.M. Kamchatnov, Institute of Atomic Energy imeni I.V. Kurchatov]

[Abstract] Propagation of periodic femtosecond pulses through nonlinear optical fibers is analyzed on the basis of a generalized nonlinear Schroedinger equation which, unlike that for picosecond pulses, describes the evolution of a pulse envelope without the simplifying assumption of a quasi-steady nonlinear response. The analysis is simplified, however, by assuming a simple relation between the periodic solutions to this equation and the solutions to another integral one, namely the "nonlinear Schroedinger equation with a derivative". Its integrability derives from the fact that it formulates the condition for compatibility of two systems of linear equations containing the spectrum parameter λ. Following an analysis of those periodic solutions, Whitham modulation equations are constructed in the diagonal Riemann form by the inverse problem method for a description of nonhomogeneous solutions and determination of the spectrum parameters λ_i, which in turn determine the periodic solutions. For illustration, these Whitham equations are applied to evolution of an oscillating-field region after a wave flip-over. The author thanks A.A. Vedonov, V.G. Nosov, A.L. Chernyakov, and V.R. Chechetkin for discussing the results. References 23.

Solitons on Dynamic Domain Wall in Ferromagnet

907J0002B Moscow ZHURNAL EKSPERIMENTALNOY I TEORETICHESKOY FIZIKI in Russian Vol 97 No 1, Jan 90 pp 337-342

[Article by M.V. Chetkin, I.V. Parygina, V.B. Smirnov, and S.N. Gadetskiy, Moscow State University imeni M.V. Lomonosov]

[Abstract] Clusters of vertical Bloch lines moving in different directions on the wall between two domains in a ferrite garnet were recorded in real time by the method of double high-speed photography. They were recorded for an analysis of their evolution and collision kinetics within the duration of a magnetic field pulse which causes movement of the domain wall and attendant action of the gyroscopic force which moves the Bloch clusters with that wall. Two light pulses were sent into a ferrite garnet crystal, one after the appropriate lay, with the two respective polarizers oriented to form an angle equal to double the Faraday rotation angle between their principal planes and the analyzer oriented so as to make its principal plane bisect that angle. The first and second dynamic positions of the domain wall with a Bloch cluster appeared on the photographic film as light-to-dark and dark-to-light transitions. With the domain wall moving slowly 10-20 m/s, two LGI-21 lasers pumping a rhodamine-6G cell were needed to ensure the necessary 0.5-1 μs optical time interval between two light pulses of 8 ns duration. An analysis of the photographs, supported by numerical data on relaxation of domain wall flexure (the relaxation time being proportional to the mobility and inversely proportional to the magnetic field gradient) reveals that two clusters of vertical Bloch lines with equal amplitudes but opposite topological charges annihilate each other through a breather colliding collinearly. The breather relaxes within the same relaxation time, or penetrate each other in a soliton manner without change of amplitude and velocity when the velocity of the domain wall is high. Figures 5; references 14.

UDC 535.317

Femtosecond Light Echo and Associative Space-Time Holography

907J0003A Moscow IZVESTIYA AKADEMII NAUK SSSR: SERIYA FIZICHESKAYA in Russian Vol 53 No 12, Dec 90 pp 2299-2304

[Article by A.K. Rebaniye, Institute of Physics, ESSR Academy of Sciences]

[Abstract] Use of cryogenic extrinsic media with photoburning of persistent spectral holes for high-volume high-density optical data recording is considered. The coherent optical response of such a medium to resonant excitation by a sequence of ultrashort laser pulses is a photochemical buildup of a stimulated light echo. The principle of space-time holography has been extended to associative hologram recording in such a medium, this method not requiring use of reference pulses. In an experiment concerning the feasibility of this scheme, a double-stream ring dye laser with colliding beams and a four-prism dispersion compensator served as the source of femto-second pulses of 620 nm light within a 150-250 cm^{-1} wide line tunable over the 610-630 nm range. Tests were performed with 0.7 mm thick polystyrene plates containing 0.0001-0.001 mol.% octaethyl porphin or protoporphyrin as impurity for photoburning of spectral holes, the plates being placed in a helium immersion cryostat. The structure of spectral holes was recorded in such a plate by letting two laser beams with a small angle between them merge in it within a spot 2 mm in diameter. Both lasers were pulsed at a repetition rate of 110 MHz, pulses from one laser delayed by a time interval much shorter than the repetition period but much longer than the pulse duration. Photoburning was exposed within 100 s after irradiation with a dose of 100 mJ/cm^2. Photochemical buildup of a stimulated light echo was recorded in the cross-correlation scheme with the aid of a $LiIO_3$ crystal serving as a second-harmonic generator, a part of the laser output power being diverted into reference pulses. The test results , supported by a theoretical analysis of the process, indicate that associative holography with femtosecond light echo pulses in such a medium ensures a more complete dispersion of

data over the spectral memory as well as a better correlation and coincidence of signals with the key fragments of an image during recording and readout than does conventional holography. The author thanks coauthors of the experimental part Ya. Aaviksoo, R. Kaarli, and Yu. Kul, also thanks Academician K.K. Rebaniye for discussing the subject of an associative spectral memory. Figures 3; references 22.

UDC 535.4

Reconstruction of Image From Reflection Hologram Recorded Without Homocentric Reference Beam

907J0016A Kiev UKRAINSKIY FIZICHESKIY ZHURNAL in Russian Vol 35 No 3, Mar 90 pp 353-356

[Article by P.V. Polyanskiy, Chernovtsy University]

[Abstract] Reconstruction of an image representing an entire scene with high luminance fidelity from an amplitude or phase reflection hologram with an arbitrary ratio of readout and blank areas by spatial separation of diffraction orders is considered, reconstruction of a conjugate (with respect to the reference source) image without distortion of the luminance distribution is shown to be possible without use of a quasipoint reference source. This is demonstrated by an analysis of the process of reading out, by means of the object field, a hologram on which there has been recorded a luminance distribution describable by an operator of the [begin set] $T_0+(T_1+R)|G+Q|^2$ [end set] form. Such an operator transforms the reading field of complex amplitudes into a diffraction field. A partial operator of the [begin set] $T_0+T_1G^*G$ [end set] form then reconstructs the phantom image G^* of an object G within the region in which the latter is localized, while diffraction of the reading field by the RG^*Q component of the hologram structure reconstructs the real image for viewing on a screen. The theoretical feasibility of such an image reconstruction, with the field reflected by the mirror acting as the reference field, has been confirmed by an experiment. Figures 2; references 3.

UDC 535.345.6

Formation of Ultrashort Light Pulses With Aid of Filters Synthesized by Burning of Spectral Holes

907J0039B Tallinn IZVESTIYA AKADEMII NAUK ESTONII: FIZIKA, MATEMATIKA in Russian Vol 39 No 1, Jan-Mar 90]

[Article by Heiki Sonajalg, Institute of Physics, ESSR Academy of Sciences]

[Abstract] The feasibility of forming ultrashort light pulses with the aid of filters which have been synthesized by burning spectral holes is examined theoretically. A functional relation is established between the spectral response characteristic and the transmission spectrum of such a filter in the form of a plate containing photochromic impurity centers with a nonuniformly broadened absorption band. Each center is described as a harmonic oscillator of an electric dipole and propagation of light through such a medium is described by a first-order differential equation. Shaping an optical pulse is shown to be possible by controlling the spectral density of those centers and thus the shape of the filter response curve. The two constraints on the spectral density function of those centers are that it cannot have any strong singularity inasmuch as the width of their uniform absorption lines is finite and that it cannot become infinitely large so as to make the transmission coefficient of the filter zero at any frequency. Shaping an optical pulse is thus shown to require an analytic continuation of its Fourier transform on the complex frequency plane preferably without zeros in the lower half-plane. The procedure is demonstrated on responses of two or three fictitious optical systems to an incoming echo, responses which consist of respectively two or three attenuated and successively delayed repetitions of that echo. When there are zeros in the lower complex half-plane, it becomes necessary to find a realizable response as close as possible to the desired one. Article was presented by P. Saari. The author thanks P. Saari for formulating the problem and for support, R. Kaarli, J. Kikas, and J. Aaviksoo for helpful discussions. Figure 2; references 19.

UDC 621.373.826

Dynamics of Nonlinear Rotating Light Waves: Hysteresis and Interaction of Wave Structures

907J0041C Moscow KVANTOVAYA ELEKTRONIKA in Russian Vol 17 No 4, Apr 90 pp 391-392

[Article by S.A. Akhmanov, M.A. Vorontsov, and A.V. Larichev, Moscow State University imeni M.V. Lomonosov]

[Abstract] An experimental study of nonlinear rotating light waves was made, for the purpose of which an optically controllable liquid-crystal transparency with cubic optical nonlinearity and with a refractive index $n = n_0+n_2I$ linearly dependent on the light intensity had been placed inside a ring cavity. The topology and the spatial scale of transverse interaction were varied by means of a field transformer in the feedback loop. Multilobar optical reverberator structures were generated by means of a fiber optic rotation transformer and a set of masks, the latter facilitating extraction of thin annular layers. Spiral waves were generated by appropriate variation of the transverse spatial scale through compression or expansion. The controllable variables in the experiment were the angle of field rotation in the feedback loop, the wave nonlinearity factor, and the diameter of an annular layer. Measurements have revealed a dependence of the angular velocity of rotating wave structures on the field rotation angle, this dependence being characterized by bipolar hysteresis. The results of this experiment are

compared with and found to agree closely with a quantitative theory of rotating wave structures. This theory was developed by the authors on the basis of a second-order nonlinear differential equation with a cosine term which describes the nonlinear response of a nonlinear diffusive medium to large-scale transverse interaction as a result of field rotation as well as small-scale quasi-local interaction. Figures 3; references 8.

Evolution of Dark Solitons From Stimulated-Raman-Scattering Noise

907J0044D Leningrad PISMA V ZHURNAL TEKHNICHESKOY FIZIKI in Russian Vol 16 No 6, 26 Mar 90 pp 25-29

[Article by S.A. Gredeskul and Yu.S. Kivshar, Institute of Low-Temperature Engineering Physics, UkSSR Academy of Sciences, Kharkov]

[Abstract] Formation of dark optical solitons during stimulated Raman cascade scattering of light in optical fibers is considered, with such solitons or stationary gaps in the envelope of light pulses forming in optical fibers with positive chromatic dispersion. The possibility and inevitability of quasi-stationary picosecond dark soliton-like pulses evolving from stimulated-Raman-scattering noise is demonstrated by a theoretical analysis of the decay of a noise-like long Stokes pulse within a fiber segment with positive dispersion. The results of this analysis, based on the nonlinear Schroedinger equation for the linear scattering problem, can be interpreted physically, namely that this is how the central peak of the autocorrelation function for radiation emission by stimulated Raman scattering is formed. The authors thank V.N. Serkin for discussion. Figures 1; references 10.

Time-Resolved Picosecond Photon Echo in Array Natural Excitations of Medium (Mixed $CdSe_xS_{1-x}$ Crystals)

907J0045B Moscow PISMA V ZHURNAL EKSPERIMENTALNOY I TEORETICHESKOY FIZIKI in Russian Vol 51 No 7, 10 Apr 90 pp 361-364

[Article by G. Noll. U. Ziegner, and E. Goebel, Marburg University (West Germany), S.G. Shevel, Institute of Physics, UkSSR Academy of Sciences]

[Abstract] A photon echo was for the first time unambiguously extracted with picosecond time resolution from an array of natural excitations in a medium, namely in mixed $CdSe_xS_{1-x}$ semiconductor crystals. Such crystals in the form of up to 50 μm thick petals had been grown from the gaseous phase. Measurements of both spontaneous and stimulated photon echo were made at temperatures about 10 K, with a tunable rhodamine 6G laser as excitation emitting light pulses of 7 ps duration at a repetition rate of 500 kHz while being synchronously pumped by second-harmonic radiation from a YAG:Nd^{3+} master laser. The photon echo was recorded in a high-speed optoelectronic camera by synchronously scanning the medium with a charge-coupled-device target with a 20 ps time resolution. Data on a $CdSe_{0.6}S_{0.4}$ specimen indicate that the transmission coefficient for light pulses increases as the energy of excitation pulses is decreased. Considering that excitons bound to fluctuations of the crystal potential, rather than free excitons determine the optical properties of the medium, evidently these excitons, unlike free ones, are not subject to dephasing by interparticle collisions. The data also reveals a saturation of the photon echo, evidently owing to saturation of the resonance states of those bound excitons. The results of this study are reasonably consistent with theoretical predictions based on the effects of disorder and Anderson localization. Figures 2; references 15.

UDC 537.312.62

Detection of Microwave Radiation With Regular Three-Dimensional Array of Josephson Junctions

907J0048B Leningrad FIZIKA TVERDOGO TELA in Russian Vol 32 No 1, Jan 90 pp 321-323

[Article by V.N. Bogomolov, V.V. Zhuravlev, Yu.A. Kumzerov, V.P. Petranovskiy, S.G. Romanov, and L.V. Samoylovich, Institute of Engineering Physics imeni A.F. Ioffe, USSR Academy of Sciences, Leningrad]

[Abstract] Use of a regular three-dimensional array of identical Josephson junction as microwave radiation detector is examined, one-dimensional and two-dimensional arrays already being used and their performance characteristics known. Such an array can be produced by the matrix method of filling voids in a dielectric matrix with small particles so as to form a configuration of links compatible with the matrix structure. Such arrays were produced experimentally by densely pressing a lot of identical silicate globules about 250 nm in diameter into molds for manufacture of synthetic opals. This forms macroscopic close-packed hexagonal or face-centered cubic lattices and then fills the voids, approximately 25% of the total volume, with Pb, In, Sn, or Bi-Pb melt under pressure so as to form multiply-linked structures with interleaving about 120 nm large particles in octahedral interstices and about 50 nm large particles in tetrahedral ones, all interconnected by about 25 nm bridges. The dimensions of these detector structures were 1x1.5x3 mm^3 and each contained up to 10^{12} identical weak-link bridges. Their response to microwave radiation at 4.2-2.5 K temperatures was measured without a matching device, the carrier frequency being varied over the 0.4-10 GHz range and its amplitude being modulated to a depth of approximately 20 dB by a 330 Hz alternating current to be detected by the Josephson junction arrays. The detector response current was measured over a range of microwave input power up to complete suppression of superconductivity (typically 5 mV), this current being found to pass through several discrete peaks within that range. The relative magnitude of its maxima, but not the

voltages corresponding to them, were found to depend on the microwave frequency. The current-voltage characteristics of these detectors was measured by the four-point method. They were found to be those of superconductor junctions, but blurred by thermal fluctuations and with neither the current step, typical of single junctions, nor other obvious singularities. Figures 2; references 4.

New Method of Predicting Proneness of Coals to Outbursts

907J0049C Leningrad PISMA V ZHURNAL TEKHNICHESKOY FIZIKI in Russian Vol 16 No 5, 12 Mar 90]

[Article by A.N. Gubkin, P.P. Zaytsev, V.A. Zagoruyko. Ye.M. Panchenko, O.I. Prokopalo, and G.D. Frolkov]

[Abstract] A new method of predicting proneness of coals to outbursts is proposed, this method being based on the recently discovered electretic state and on the marked differences between the characteristics of that state in safe and hazardous coal deposits respectively. Experiments leading to this discovery were performed on coals from three deposits where outbursts had occurred and from sites where outbursts had never been observed. The specimens were tested in a Minsk-12m electron-paramagnetic-resonance spectrometer, after they had been pulverized and the powders then compacted into 1.5 mm thick disks 8 mm in diameter. As indicators of differences between safe and hazardous coals have been selected the electretic potential representing the magnitude of electretic charge and the thermally induced depolarization current representing the rate of relaxation of the electretic state. Specimens were electrically polarized through two metal electrodes at room temperature in an electrostatic field of 11-13 V/cm intensity, the electretic potential then being measured by the compensation method and the depolarization current being measured in the short-circuit mode. An analysis of the data reveals a correlation between each indicator and the proneness to outbursts: the higher the depolarization current and the lower the electretic potential difference is, the greater the danger of outbursts. Tables 1; references 7.

UDC 537.876:517.958

Information Content of Transform of Functions and Possibility of Detecting Systematic Errors in Solution of Ill-Conditioned Problems

907J0051B Moscow DOKLADY AKADEMII NAUK SSSR in Russian Vol 311 No 3, Mar 90 pp 601-606

[Article by A.G. Pavelev, Institute of Radio Engineering and Electronics, USSR Academy of Sciences, Fryazino (Moscow Oblast)]

[Abstract] Necessary and sufficient conditions for the existence and uniqueness of a minimally unstable solution to an ill-conditioned problem such as approximation of experimental data with integrable analytic piecewise-continuous analytic functions are established on the basis of three theorems. These also validate the use of transforms of such functions for detection of systematic errors in that solution and regularization of the latter. Transforms of five functions serve as illustration: the Laplace transform L(p) used in radiophysics and for reconstruction of altitudinal temperature profile on the basis of atmospheric radiation measurements, the k(s) transform and its generalized form for inverse problems of refraction, and the two $L_c(y)$ and $L_s(y)$ transforms for the inverse problem of atmospheric sounding based on the absorption lines of gases which make up the air. Article was presented by Academician Yu.V. Gulyayev. References 10.

UDC 533.9.01

Erosion of Relativistic Electron Beam in High-Conductivity Channel

907J0004A Moscow FIZIKA PLAZMY in Russian Vol 16 No 3, Mar 90 pp 370-375

[Article by L.V. Glazychev and G.A. Sorokin, Moscow Institute of Radio Engineering, USSR Academy of Sciences]

[Abstract] Erosion of an axisymmetric sub-Alfven short-pulse relativistic electron beam in a channel with high electrical conductivity is analyzed, taking into account, not only nonuniformity of injection and attendant transient processes, but also finiteness of the beam width, azimuthal velocity of electrons, and their scattering in the channel. A mathematical model of relativistic electron beam dynamics is constructed which includes buildup of electrical conductivity in the channel medium by such a beam, but assuming a uniform in space and constant in time electrical conductivity of the plasma. The model is based on applicable Maxwell equations for a beam-plasma system, reducible under the given conditions to a single one for the longitudinal z-component of the electromagnetic vector potential in the Lorentz gauge. This equation, put in dimensionless form by appropriate normalization of the independent variables and with the current for specificity assumed to vary sinusoidally in time, is solved for the beam as an array of macroparticle layers, moving one after another in equal intervals. Calculations on this basis yield an expression for the beam erosion rate which takes into account the scattering of electrons but is otherwise approximate only. According to it, the erosion rate within the quasi-equilibrium region is almost independent of the electrical conductivity of the channel medium. Figures 3; references 15.

UDC 533.95

Nonlinear Excitation of Surface Electromagnetic Waves on Thin Plasma Films by Light Beam

907J0004B Moscow FIZIKA PLAZMY in Russian Vol 16 No 3, Mar 90 pp 324-331

[Article by A.A. Zharov, Institute of Applied Physics, USSR Academy of Sciences]

[Abstract] Excitation of surface electromagnetic waves on thin plasma films with an initially very low permittivity ε_0 by a light beam is considered. This light beam creates "pockets" of nonlinear permittivity in the film which transform incident waves into surface electromagnetic ones. The problem is analyzed for a plasma film on an ideally conducting substrate and an obliquely incident p-polarized plane beam of electromagnetic waves with a normal electric field component E_z much larger than its tangential one E_x, the plasma film becoming dielectrically nonlinear: $\varepsilon = \varepsilon_0+\alpha|E_z|^2$. The thickness of the plasma film is much smaller than the wavelength of the incident light and the width of the light beam is much larger. The transverse magnetic field component H_y is assumed to have a Gaussian distribution, which determines the distribution of the electromagnetic field in toto. The system of three wave equations for the three field components E_x, E_z, and H_y interacting in the film, assuming an adiabatically slow incidence of the light beam, is solved by means of a Fourier transformation with respect to the x-coordinate and so as to satisfy the boundary conditions of the problem. Analysis and evaluation of the results, following a sub- inverse Fourier transformation, demonstrate that nonlinearization of the plasma film occurs through the mechanism of its optical bistability. The author thanks I.G. Kondratyev, V.V. Kurin, V.Ye. Semenov, and A.I. Smirnov for discussions and comments. Figures 7; references 8.

New Essentially Nonlinear Surface Modes at Plasma-Vacuum Interface

907J0007C Moscow PISMA V ZHURNAL EKSPERIMENTALNOY I TEORETICHESKOY FIZIKI in Russian Vol 51 No 5, 10 Mar 90 pp 261-263

[Article by N.B. Aleksic, Institute of Physics, Belgrade/ YUGOSLAVIA/, Yu.M. Aliyev and A.A. Frolov, Institute of Physics imeni P.N. Lebedev, USSR Academy of Sciences]

[Abstract] Considering that the field of sufficiently strong p-polarized surface electromagnetic waves can have a singularity within the vicinity of plasma resonance, where nonlinearities of a plasma become significant already at low power levels. It is demonstrated that new essentially nonlinear surface modes within this frequency range can appear at the plasma-vacuum interface and the threshold intensity of the electromagnetic field for appearance of these modes is subsequently determined. Calculations are based on steady-state solutions to nonlinear field equations for surface waves for boundary conditions of continuous tangential field components

$$E_x = 0 \text{ and } B = B_y = 0$$

at the plasma-vacuum interface. In the case of a plasma with a high linear permittivity component and a striction nonlinearity with saturation characterized by an exponential field dependence of the total plasma permittivity, these solutions describe retarded surface electromagnetic waves within the Langmuir frequency range, if the possibility of discontinuous plasma-field distributions disregarding spatial dispersion of these waves is admitted. The dispersion equation for these new surface modes describes an anomalous dispersion law, their propagation being possible only when the frequency-dependent intensity of their field lies within a finite range between two, upper and lower, frequency-dependent limits. The authors thank V.P. Silin for helpful discussion. References 7.

Compound Autosolitons in Gaseous and Semiconductor Plasmas

907J0028C Leningrad ZHURNAL TEKHNICHESKOY FIZIKI in Russian Vol 60 No 2, Feb 90 pp 8-13

[Article by V.V. Gafiychuk, B.S. Kerner, V.V. Osipov, and A.G. Yuzhanin, Institute of Application Problems in Mechanics and Mathematics, UkSSR Academy of Sciences, Lvov]

[Abstract] Formation of compound autosolitons in an electron-hole semiconductor plasma and their further evolution in a plasma which heats up are analyzed. That is considering, in such a plasma, the characteristic length of path for electron cool down is much shorter than the path for bipolar charge carrier diffusion. The basis for this analysis are two partial differential equations of balance describing the simultaneous kinetics of carrier concentration n (pressure P = nT) and average carrier energy (temperature T) distributions in the one-dimensional model. These equations are applied to a homogeneous electron-hole plasma with equal electron and hole concentrations, its density assumed to be sufficiently high so that the momentum imparted by a transverse electric field to the charge carriers become dissipated in electron-hole collisions. The results of numerical simulation on this basis indicate that in the case of a low lattice temperature T_L far below the Debye temperature, a hot autosoliton can be generated at temperatures from T_L to $2T_L$ and a cold one can be generated at temperatures equal to or higher than $4.542T_L$, an electron-hole plasma being stable within these two temperature ranges. Within the hotter temperature range, a cold autosoliton can be generated by a momentary local increase of the rate of charge carrier generation. This autosoliton can be a simple solitary and can be a mirror-symmetric or asymmetric compound, depending on the distance in space between successive square excitation pulses. Compound autosolitons were tested numerically for stability during finite plasma fluctuations. As the dispersion of fluctuations was increased, such an autosoliton was found to gradually lose stability and to transform into another compound, one of a different form. Asymmetric and symmetric hot compound autosolitons can be generated in an electron-hole plasma within the lower temperature range, a simple solitary one vanishing here in a sufficiently strong electric field. This pattern of of autosoliton evolution in an electron-hole semiconductor plasma is similar to that in a gaseous plasma, where the characteristic length of path for electron cool down is larger than the length of path for bipolar charge carrier diffusion. Figures 3; references 16.

UDC 533.951

Drift of Laser Plasma in Transverse Magnetic Field

907J0042A Moscow FIZIKA PLAZMY in Russian Vol 16 No 4, Apr 90 pp 415-423

[Article by Yu.A. Bykovskiy, V.P. Gusev, Yu.P. Kozyrev, I.V. Kolesov, V.B. Kutner, A.S. Pasyuk (deceased), and V.D. Peklenkov, Moscow Institute of Engineering Physics and Joint Institute of Nuclear Research]

[Abstract] An experimental study of a laser plasma in a transverse magnetic field was made concerning the drift of such a plasma under conditions corresponding to small ratios of gas kinetic pressure to magnetic pressure $\beta = (n_i m_{ii}^{2}/2\mu_9) << 1$ (n_i, m_i, and $_i$ denoting ion concentration, ion mass, and average ion velocity in the plasma, B denoting magnetic induction, and μ denoting magnetic permeability) in a cyclotron. The experiment was performed with various target materials (C,Al,Ti,Ta) under a vacuum of 10^{-5} torr and with a pulsed transverse-excitation CO_2 research laser emitting 10.6 μm radiation in double-hump pulses with an energy of 6 J contained in the two humps of 60 ns and 500 ns duration respectively. The radiation was focused by a NaCl lens for oblique incidence onto the target and so that a maximum energy density of approximately 3.10^{10} W/cm^2 could be attained. Also an LTIPCh-4 commercial laser emitting 1.06 μm radiation in pulses of 60 mJ energy and 12 ns duration was used in the experiment, an energy density of approximately 5.10^9 W/cm^2 having been attained with this laser. The uniform magnetic field was varied to a maximum intensity of 0.5 T. Plasma, backscattered by the target, was caught by a circular array of collectors at a constant negative potential of -200 V, a fine-mesh grid at ground potential having been placed in front of them. The distance from target to collectors was varied over the 1-11 cm range. Measurements and oscillograms have yielded data on the structure of plasma clusters in terms of ion currents, kinetics of plasma expansion, and on its energy characteristics. An evaluation of the data is supplemented with a theoretical analysis of plasma cluster injection into a transverse magnetic field and the resulting drift of such a cluster. This analysis is based on the solution of the equation of plasma motion in the adiabatic approximation. The authors thank Academician G.N. Flerov, and Yu.Ts. Oganesyan for support, S.L. Bogomolov, S.B. Tomilov, and A.A. Yeropkin for collaboration. Figures 10; references 42.

UDC 537.872.31

Spectral Correlation Characteristics of Spherical Electromagnetic Wave in Turbulent Plasma

907J0042B Moscow FIZIKA PLAZMY in Russian Vol 16 No 4, Apr 90 pp 430-435

[Article by V.G. Gavrilenko, M.N. Krom, and S.S. Petrov, Gorkiy State University imeni N.I. Lobachevskiy]

[Abstract] Propagation of a spherical electromagnetic wave across a flowing cold nonrelativistic, randomly nonhomogeneous plasma without a magnetic field is analyzed in the Born approximation, assuming that the wavelength is smaller than the scale of plasma turbulence due to random nonhomogeneity and disregarding effects

of depolarization. The integral scalar equation for Fourier components of the electric field of such a wave is derived from an expression for the current and then solved for the case of a monochromatic source located inside the turbulent wave-scattering plasma region. The space-time spectrum of the electromagnetic field is obtained by statistical averaging of the scattered component, only forward scattering being considered here, whereupon integration and subsequent inverse Fourier transformation of that spectrum yield the sought power spectrum in the time domain. These operations are performed for the low-angle approximation, which simplifies subsequent calculations. Scattering of isotropic spherical waves is then considered first, special cases being waves which propagate quasi-transversely and quasi-longitudinally, relative to the direction of plasma flow. Next, the directional source is considered which emits a spatially nonuniform spherical wave and the effect of that nonuniformity on the spectral characteristics of its radiation field scattered by the plasma stream. The fluctuation parameters of a directional spherical wave propagating through a plasma stream with multiple scattering are obtained by the perturbation method, this being the case of wide phase fluctuations and a Gaussian frequency spectrum with the maximum shifted, relative to the carrier frequency. The effect of plasma flow on the amplitude-frequency correlations is then evaluated in the approximation of geometrical optics in terms of the ${}_1\chi_1$ parameter, which in turn depends on the radiation pattern of the wave source, (^{2} denoting the frequency dispersion or mean-square fluctuation of its instantaneous local value). The authors thank N.S. Stepanov for helpful discussion. References 7.

UDC 533.9.01

Analysis of Injection of Relativistic Electron Beam Into Neutral Gas on Basis of Numerical Model

907J0070A Moscow FIZIKA PLAZMY in Russian Vol 16 No 5, May 90 pp 592-598

[Article by L.V. Glazychev and G.A. Sorokin, Moscow Institute of Radio Engineering, USSR Academy of Sciences]

[Abstract] A model is constructed for numerical analysis of the injection of a relativistic electron beam into a neutral dense gas and its subsequent propagation through that medium with attendant erosion by loss of charge. The model, in the approximation of an axisymmetric beam with paraxial trajectories of beam particles and with a smooth current rise, treats a beam pulse as a series of successive periodically injected clusters of many "large" identical charge carrying particles. It contains three sets of equations: equations of motion for macroparticles whose longitudinal velocity normalized to the speed of light is assumed to remain constant, equations of electrodynamics simplified by assuming that the time constant of current rise, i.e., duration of a current pulse is much longer than the light travel time across the beam, and equations of plasma-chemical kinetics. Numerical solution of this transient-state problem with the gas pressure varied over the 2-700 torr range has yielded data not only on the distance dependence of the beam front velocity and the pressure dependence of the beam current compensation factor, but also on both distance and pressure dependence of the energy transfer to the gas, its Joule heat component, and energy loss in the chamber walls. The results agree overall with the results of an experiment performed on the Terek-1R accelerator and with those of other experiments, except for the results of theoretical energy calculations which do not account for possible asymmetric beam instabilities.

Evolution of Electron Beam in Reverse Plasma Maser Effect

907J0070B Moscow FIZIKA PLAZMY in Russian Vol 16 No 5, May 90 pp 599-603

[Article by S.V. Vladimirov and V.S. Krivitskiy, Institute of General Physics, USSR Academy of Sciences]

[Abstract] Evolution of a monoenergetic electron beam in a turbulent plasma interacting simultaneously with longitudinal resonance and nonresonance waves is analyzed. It is analyzed in the one-dimensional approximation of a plasma in a strong external magnetic field and with the cyclotron frequencies of electrons (ions) much higher than their plasma frequencies. The resonance waves are assumed to be of the Langmuir kind and the nonresonance waves are treated as ion-acoustic ones, all propagating exactly in the direction as if the cyclotron frequencies of electrons were infinitely high. The collision integral is derived, considering quasi-linear interaction of resonance waves with, and their scattering by, plasma particles is here accompanied by nonlinear interaction of plasma particles with nonresonance waves which satisfy neither the condition of Cerenkov resonance nor the condition of scattering resonance with resonance waves. The collision integral then yields the plasma particle distribution function and its rate of change as the difference between a quasi-linear diffusion component and a nonlinear diffusion component, the latter exceeding the former during the initial relaxation period and at the tails of the beam particle distribution. References 3.

Effect of Al and In Impurities on Superconductivity of 2212-Phase Bi-Sr-Ca-Cu-O Material

907J0008B Leningrad PISMA V ZHURNAL TEKHNICHESKOY FIZIKI in Russian Vol 16 No 4, 26 Feb 90 pp 32-36

[Article by Ye.M. Gololobov, N.A. Prytkova, Zh.M. Tomilo, D.M. Turtsevich, M.S. Tseluyevskiy, and N.M. Shimanskaya, Institute of Solid-State and Semi- conductor Physics, BSSR Academy of Sciences, Minsk]

[Abstract] An experimental study of the 2212-phase $Bi_2Sr_2CaCu_2O_y$ superconductor material for thin-film devices was made with Al_2O_3 and In_2O_3 intentionally added as impurities, to simulate infusion of Al_2O_3 substrate material and of indium from cryogenic contact tabs in such devices. Specimens of $Bi_2Sr_2Al_xCaCu_2O_y$ and $Bi_2Sr_2In_xCaCu_2O_y$ materials with x = 0.0-5.0 were produced from mixtures of fine-disperse Bi_2O_3, Al_2O_3 or In_2O_3, CuO, $SrCO_3$, $CaCO_3$ powders by solid-state synthesis reaction at 800-870°C temperatures in air. They were examined in a DRON-3 x-ray diffractometer with a CuK_α- radiation source for phase composition and in an x-ray microlocal spectrum analyzer for distribution of impurity atoms. While the 2212 phase was found to remain the dominant one, pure aluminum rather than Al_2O_3 appeared, and in larger amounts, as more of the latter was added to the original mixture but In_2O_3 together a new In-phase appeared also in larger amounts as the indium content increased. The impurity atoms were found to settle mostly on grain boundaries and, in limited quantities, penetrate the $Bi_2Sr_2CaCu_2O_y$ crystal lattice, indium being less soluble than aluminum. The temperature dependence of the electrical resistance, based on measurements covering the 4.2-300 K range, indicates that addition of aluminum up to x = 2.0 lowers the end point of superconducting transition from about 70 K (x = 0) to about 40 K (x = 2.0), the dR/dT slope decreasing as the aluminum content is increased and superconductivity is replaced by non-metallic behavior as the aluminum content is increased further. Addition of indium had a similar but stronger effect, the end point of superconducting transition dropping faster as the indium content was increased up to x = 1.0 and then along a more intricate path to 30 K when x = 2. Some specimens with indium did not become superconducting even at 4.2 K. Figures 3; references 7.

UDC 538.248:537.312.62

Contactless Measurements of Critical Current in Superconductor Plates and Films

907J0015A Leningrad FIZIKA TVERDOGO TELA in Russian Vol 32 No 2, Feb 90 pp 379-383

[Article by M.P. Petrov, M.V. Krasinkova, Yu.I. Kuzmin, and I.V. Pleshakov, Institute of Engineering Physics imeni A.F. Ioffe, USSR Academy of Sciences, Leningrad]

[Abstract] Contactless magnetic measurement of current in superconductors for a determination of the critical current density is proposed, the method being suitable for thin films as well as for bulky material and particularly applicable to type-II superconductors with pinning centers. Measurements are made with a Hall probe and the critical current density is determined from the width of the hysteresis loop. The theory of this method is based on the Bean-London equation with both saturation and shielding taken into account. It was tested on a disk with a 4.1 mm radius made of $YBa_2Cu_3O_{7-d}$ ceramic, its diameter-to-thickness ratio being varied from 1 to 10,000 by face grinding which decreased its thickness in discrete steps. The object was to determine the dependence of the loop width and thus of the critical current density on that ratio as well as on the magnetic field intensity, on the basis of measurements made at 77 K temperature. It was also tested on a disk 3.5 mm thick with a 5.1 mm radius made of $Tl_2Ba_2Ca_2Cu_3O_x$ ceramic, the object being to determine the field dependence of the critical current density and of the pinning force on the basis of measurements made at 110 K temperature with the critical current density. This specimen had been prepared from a mixture of Tl_2O_3, $BaCuO_2$, Ca_2CuO_3 powder mixture by synthesis at 700°C in air, followed by compaction of the product and annealing of the latter at various temperatures, evaporation of Tl_2O beginning at 900°C and this temperature thus having been found to be the optimum one. Figures 4; references 12.

UDC 537.311.322

Anisotropy of Charge Carrier Scattering in $Bi_2Te_{3-x}Se_x$ and $Bi_{2-y}In_yTe_3$ Solid Solutions

907J0015B Leningrad FIZIKA TVERDOGO TELA in Russian Vol 32 No 2, Feb 90 pp 488-492

[Article by V.A. Kutasov and L.N. Lukyanova, Institute of Engineering Physics imeni A.F. Ioffe, USSR Academy of Sciences, Leningrad]

[Abstract] The anisotropy of electron scattering in two n-type $Bi_2Te_{3-x}Se_x$ (x = 0.12, 0.3) and two n-type $Bi_{2-y}In_yTe_3$ (y = 0.06, 0.12) solid solutions is evaluated by theoretical analysis and interpretation of experimental data obtained by measuring components of the Hall-effect tensor ρ_{ijk} and the magnetoresistivity tensor ρ_{ijkl} in weak magnetic fields along with components of the electrical resistivity ρ_{ij}. The analysis is based on the multivalley model of the energy spectrum with scattering anisotropy, according to which each component of the relaxation time tensor can be expressed as the product of an isotropic function which depends on the energy only and the corresponding anisotropic multiplier (tensor component) which depends, neither on the energy nor on the direction of electron motion. With the aid of the experimental data, including available data on the Bi_2Te_3 compound, have been calculated the temperature dependence of $\rho_{11}\rho_{1133}\rho_{123}^2$ ratio for these solid solutions and its dependence on x (Se concentration) or y (Te

concentration) at 77 K, also the concentration dependence of the τ_{ij}/τ_{11} ratios of relaxation time tensor components (τ_{11}- isotropic relaxation time) and of inverse-effective-mass tensor components at 77 K. Figures 3; references 9.

UDC 533.213.1

Effect of Disorder on Superconducting Transition Temperature for Simple Amorphous Metals

907J0016B Kiev UKRAINSKIY FIZICHESKIY ZHURNAL in Russian Vol 35 No 3, Mar 90 pp 417-421

[Article by Yu.P. Krasnyy, N.P. Kovalenko, and V.F. Tsarev, Odessa Institute of Technology imeni M.V. Lomonosov for Food Industry]

[Abstract] Superconducting transition of simple amorphous metals is analyzed theoretically, considering that electron-phonon interaction is the principal mechanism of superconductivity and that the Eliashberg equations apply to amorphous metals as well as to crystalline ones. The analysis is based on a model in which the critical temperature depends only on structural changes and on changes in the phonon spectrum. Ions are assumed to be randomly distributed and to oscillate about their quasi-equilibrium positions in a simple amorphous metal. Electron-ion interaction in such a metal is characterized by a weak pseudopotential corresponding to a distorted long-range order in the phonon spectrum and consequently a diffuse scattering of electrons. Inasmuch as an exact solution to the Eliashberg equations has not yet been obtained, the critical temperature is calculated in the MacMillan approximation (PHYSICS REVIEW Vol 167 No 2, 1968) for intermediate to strong links and in the Karakozov-Maksimov-Mashkov approximation (ZHURNAL EKSPER. I TEOR. FIZIKI Vol 68 No 5, 1975) for intermediate to weak links. The critical temperature is accordingly determined by the phonon frequency and the field penetration depth, the field penetration depth being determined by the phonon frequency, both directly and implicitly, through the Eliashberg function. This function is evaluated by the perturbation method, only terms of first-order and second-order magnitudes with respect to the pseudopotential being included. Numerical values of the critical temperature, of the field penetration depth, also of the Debye temperature and thus the phonon frequency δ_{log} have been obtained for amorphous as well as crystalline Al, Mg, Zn, Sn, Pb, using the structural factor of a spherulitic body in the Perkus-Yevik (?) approximation and the Ashcroft pseudopotential, its parameter having been determined from electrical conductivity data. The authors thank I.K. Yanson and I.V. Krivoshey for interest, V.M. Adamyan and participants of the seminar held by the Department of Theoretical Physics at the Odessa University for discussion of the results. Tables 1; references 21.

Paramagnetism Five Times Stronger Than Clogston Limit in Organic Superconductor $(ET)_4Hg_{2.89}Br_8$

907J0022D Moscow PISMA V ZHURNAL EKSPERIMENTALNOY I TEORETICHESKOY FIZIKI in Russian Vol 51 No 6, 25 Mar 90]

[Article by R.N. Lyubovskaya, R.B. Lyubovskiy. M.K. Makova, and S.I. Pesotskiy, Institute of Chemical Physics, USSR Academy of Sciences]

[Abstract] An experimental study of the organic superconductor $(ET)_4Hg_{2.89}Br$ (ET denoting bis-ethylenedithio-tetrathiafulvalene) was made, for verification of the earlier discovered anomalously large $dH_{c2}{}^a/dT$ slope (approximately 100 kOe/K) of its H_{c2}-T curve within an only 50 kOe wide range of magnetic field intensity. In this study, the upper critical magnetic field along the a-axis, also along both b' and c* axes, was measured in external magnetic fields of up to 150 kOe intensity at temperatures from 300 K to 2 K. The electrical resistivity of rhomboidal single crystals along the a-axis was 0.1-0.5 ohm.cm at 300 K and dropped by a factor of 5-10 at 4.3 K, at which temperature superconducting transition had occurred. The upper critical magnetic field along the a-axis was found to be approximately equal to that along the b'-axis and much higher than along the c*-axis. An analysis of the data according to the Bardeen-Cooper-Schrieffer theory indicates a paramagnetism at near zero temperature three times stronger than the Closton limit in the weak field approximation and five times stronger when augmented by the orbital effect. Such a strong paramagnetism is hardly attributable to triplet pairing but rather to the possibility of very strong electron pairing as well as to weak paramagnetism suppressing spin-orbital interaction, this interaction being usually strong in "dirty" superconductors but not in this particular one. The authors thank N.Ye. Alekseyevskiy and T. Palevskiy for support, A.V. Zvarykin and A.G. Khomenko for assistance in performing the experiment, L.N. Bulayevskiy, N.F. Shchegolev, and V.N. Laukhin for helpful discussions. Figures 2; references 9.

Self-Propagating High-Temperature Synthesis of High-T_c Superconductors

907J0026C Moscow DOKLADY AKADEMII NAUK SSSR in Russian Vol 311 No 1 Mar 90 pp 96-101

[Article by A.G. Merzhanov, I.P. Borovinskaya, M.D. Nersesyan, A.G. Peresada, and Yu.G. Morozov, Institute of Structural Macrokinetics, USSR Academy of Sciences, Chernogolovka (Moscow Oblast)]

[Abstract] A new method of synthesizing various substances has been developed particularly suitable for producing high-T_c superconductor materials and based on self-propagating high-temperature chemical interaction of component substances. The scheme of such a synthesis is "combustible metal + oxidizing peroxide condensate + gaseous oxidizer + active oxide filler =

high-T_c superconductor + heat". All known superconductors of this class such as Y(RE)-Ba-Cu-O and other ceramics have already been produced by this method from powder mixtures of the respective reactants, with the oxygen pressure varied over the 0.1-1.0 MPa range. The synthesis is effected in a wave fashion by the propagating combustion front of a flame originating in the burner nozzle. The process was monitored, for an evaluation of the temperature profile and the reaction rate. The products were analyzed chemically, by the iodometric method for oxygen content, and were examined metallographically including x-ray phase and x-ray structural analyses. They were also tested mechanically for strength and specific surface. The data have yielded information on the various combustion and attendant reaction stages including transition from stable mode to either oscillatory or spin-type unstable mode. They also indicate that under an excessive oxygen pressure, the process stalls, which is characteristic of weakly exothermic processes involving reactants with low caloric value especially when convection increases the loss of heat and when the thermal stability of the metal oxide increases with rising ambient pressure. An analysis of structural macrokinetics reveals that near the combustion front, copper oxidizes into intermediate compounds within the first 15 s, forming cuprates and the tetragonal nonsuperconducting phase of a complex oxide, while far behind the front its oxidation is completed within the next 45-60 s with formation of the oxygen-rich orthorhombic superconducting phase. In the interesting case of 2223-phase Tl-Ba-Ca-Cu-O material, its critical superconducting transition temperature was found to be 116 K, on the basis of electrical resistivity measurements, and 90 on the basis of magnetic susceptibility measurements, the transition beginning already at 135 K. On account of its not only scientific but also practical importance, this method of synthesizing high-T_c superconductor materials needs to be organized for production. An apparatus has been built, therefore, which is capable of producing several kilograms of a high-quality $YBa_2Cu_3O_{7-x}$ superconductor material which, after a 3 h cooling period appears in the form of black cake with 40-60% porosity. Its superconducting transition occurs within a 2-4 K temperature range and is completed at 95 K. Figures 4; references 11.

UDC 538.943

Band Model of Heavy-Fermion Superconductor

907J0031A Kharkov FIZIKA NIZKIKH TEMPERATUR in Russian Vol 16 No 2, Feb 90 pp 172-183

[Article by A.S. Rozhavskiy and I.G. Tuluzov, Institute of Low-Temperature Engineering Physics, UkSSR Academy of Sciences, Kharkov]

[Abstract] A band model of heavy-fermion superconductors such as $CeCu_2Si_2$ is proposed for a phenomenological description of their thermodynamic characteristics. Their band structure is in this model, and on the basis of experimental evidence, formed by three interacting intrinsic bands: two f-bands and one s-band. While the f-bands are narrower than the interval between them and do not intersect, both corresponding to widened Kramer's atom levels, the s-band is wider than the interval between the two f-bands. The interaction Hamiltonian of this system disregards Coulomb interaction within the intrinsic bands but includes hybridizing interaction of bands which intersect; this interaction being subject to a specific dispersion law. Diagonalization of this Hamiltonian by the standard w-u-v transformation leads automatically to a BCS nonphonon Hamiltonian with one term corresponding to a singlet nonphonon superconducting state and, if the hybridization parameters include spin-orbit coupling, and also with terms corresponding to a triplet superconducting state and spin-polarized band states respectively. The density of states is calculated and relations describing the thermodynamics of the normal state are established on the basis of this model, considering that the chemical potential of the system lies within the first and second hybridized bands. These relations yield the temperature dependence of the specific heat, of the magnetic susceptibility, and of the derivative of the chemical potential with respect to temperature. The thermodynamic characteristics of the superconducting state are only estimated on the basis of the same model and the BCS theory, these estimates yielding low superconducting transition temperatures and a two-fluid state below the critical temperature. While the electrodynamic characteristics of the system are determined by the shunting superconducting component only, both components determine its thermodynamic characteristics, which may explain the power-law temperature dependence of its specific heat below the critical temperature. The authors thank I.O. Kulik for helpful discussions and D.I. Khomskiy for helpful comments. Figures 4; references 11.

UDC 536.945

Motion of Abrikosov Vortices in Thin Films

907J0031B Kharkov FIZIKA NIZKIKH TEMPERATUR in Russian Vol 16 No 2, Feb 90 pp 191-194

[Article by A.S. Melnikov, Institute of Applied Physics, USSR Academy of Sciences, Gorkiy]

[Abstract] Motion of Abrikosov vortices in a thin film of type-II superconductor material by action of a Lorentz force is examined. The energy being dissipated is not only because a superconductor film of finite thickness has a finite electrical resistivity when placed in a magnetic field normal to its surface, stronger than the lower critical, so that the motion is attended by viscous drag, but also owing to the finite length of vortex lines when their length is shorter than both electric-field and magnetic-field penetration depths. An analysis of this phenomenon, according to the phenomenological nonsteady-state Ginzburg-Landau theory, indicates that the

electrical conductivity of such films in the resistive state and in a magnetic field normal to their surface depends on the film thickness according to an inverse-logarithmic law, as long as their thickness remains smaller than the electric-field penetration depth. For a film of a given thickness, its dependence on the temperature rise above critical may depart from the power law as the critical temperature is too closely approached. The author thanks V.M. Genkin for helpful discussions. References 2.

UDC 538.945

Bolometric and Noise Characteristics of High-T_c Superconductor Structures

907J0032A Kharkov FIZIKA NIZKIKH TEMPERATUR in Russian Vol 16 No 1, Jan 90 pp 70-79

[Article by B.B. Banduryan, I.M. Dmitrenko, V.G. Yefremenko, V.Yu. Lavreshin, and G.V. Shustakova, Institute of Low-Temperature Engineering Physics, UkSSR Academy of Sciences, Kharkov, S.V. Gaponov, Z.F. Krasilnik, A.Yu. Klimov, D.G. Pavelev, and A.Yu. Churin, Institute of Applied Physics, USSR Academy of Sciences, Gorkiy]

[Abstract] Use of high-T_c superconductors for cryogenic bolometer sensing elements is considered. Examples of such elements are $YBa_2Cu_3O_{7-d}$ ceramic structures, single crystals, polycrystalline films on BaF_2 substrates, and epitaxial (single crystal) films on $SrTiO_3$). Their suitability for this application is confirmed by an analysis of experimental data and theoretical relations pertaining to their performance characteristics, namely the temperature dependence of their electrical resistance and of the critical current as well as their thermophysical properties, energy and noise characteristics. The energy characteristics of such radiation detectors and the optimum operating conditions were determined on the basis of tests for sensitivity threshold, spectral sensitivity, and response speed, with the radiation from standard sources appropriately filtered. Their current-voltage characteristics were also measured, during exposure to background radiation at 10 mW power level with the bolometer platform at various temperatures within a 0.3 K range. The temperature dependence of their integral sensitivity and determined in both the electrical resistance mode and the critical current mode. The noise power in these detectors was determined on the basis of noise voltage and noise current measurements. Noise in such devices, in addition to a thermal component and a component due to randomness of heat exchange with the ambient medium, also including a component due to current, jumps between conducting grains and local states, due to tunneling effects, percolation, and other causes. The results of these tests indicate that the excess noise, proportional to the displacement current, is not inherent and in perfect single-crystal films with grain orientation, normal to the substrate surface, can be reduced to levels not higher than that of thermal noise. Under conditions of maximum sensitivity, moreover, voltage and current fluctuations in such films are determined by fluctuations of the thermal flux. Figures 7; references 12.

UDC 538.945

Magnetic Susceptibility of Tl-Ca-Ba-Cu-O High-T_c Superconductor Ceramic

907J0032B Kharkov FIZIKA NIZKIKH TEMPERATUR in Russian Vol 16 No 1, Jan 90 pp 113-116

[Article by V.A. Ventsel, A.Ye. Petrova, and A.V. Rudnev, Institute of High-Pressure Physics imeni L.F. Vereshchagin, USSR Academy of Sciences, Troitsk (Moscow Oblast)]

[Abstract] An experimental study of the ceramic $Tl_2Ca_7Ba_3Cu_8O_7$ high-T_c superconductor material was made, the purpose being to determine the temperature dependence of its magnetic susceptibility, as well as of both lower and upper critical magnetic fields, on the basis of measurements with an alternating-current bridge in magnetic fields of up to 90 kOe intensity. Measurements were made at temperature from the critical 100 K down to 1.3 K, with a copper-constantan thermocouple over the upper range and with a carbon resistance thermometer over the lower range. The temperature inside the cryostat was regulated at rates of 100-200 K/h with heaters and helium coolant fed to the ceramic specimen through a Dewar insert. A magnetic field was produced by two current sources, either by one with a 200 A rating or by one designed for weak magnetic fields and slow rise from 0 up to 3 kOe at rates not exceeding 2 Oe/s. The magnitude of the bridge unbalance signal u, proportional to the magnetic susceptibility of the specimen, and also its waveform were found to depend on both frequency f and amplitude h of the alternating magnetic field in the measuring inductance coil. The dependence of the signal magnitude on the magnetic field in the exciting coil was found to have a singularity corresponding to the lower critical magnetic field only at measuring frequencies below 100 Hz and measuring fields weaker than 1 Oe. The temperature dependence of the lower critical magnetic field was found to follow the relation $H_{c1} = 15[1-(T/T_c)^2]$ with a maximum within 20-30 K. The temperature dependence of the upper critical magnetic field was found to be almost the same at all frequencies, with a singularity at about 50 K joining the $H_{c2} = 275(1-T/T_c)^{3.5}$ range above and the $H_{c2} =$ 440-8.4T range below. Calculations on the basis of these data and the Abrikosov relations for both critical magnetic fields have yielded two corresponding values of the Ginzburg-Landau parameter and then, disregarding the small difference between them, its temperature dependence over the same range (330 at 0 K, 8 at 100 K) with a singularity also at about 50 K. The authors thank A.A. Abrikosov for interest, Ye.P. Khlybov for supplying the specimen

Neutralization of Holes by Hydrogen in La-Sr-Cu-O Ceramic

907J0045A Moscow PISMA V ZHURNAL EKSPERIMENTALNOY I TEORETICHESKOY FIZIKI in Russian Vol 51 No 7, 10 Apr 90 pp 371-374

[Article by N.M. Suleymanov, A.D. Shengelaya, Ye.F. Kukovitskiy, and R.G. Mustafin, Kazan Institute of Engineering Physics, USSR Academy of Sciences, H. Drulis, G. Chadzynski, and J. Janczak, Institute of Low Temperatures and Structural Analysis, Polish Academy of Sciences, Wroclaw]

[Abstract] An experimental study concerning action of hydrogen injected into $La_{1.8}Sr_{0.2}CuO_4$ ceramic was made, powder specimens of this material having been produced by standard technology. After they had been held under a vacuum of 0.01 mm Hg at room temperature for several hours, pure gaseous hydrogen produced from titanium hydride was let in under a pressure of 600 mm Hg while the ceramic powder was heated at a rate of 30°C/h. The effects of hydrogen-ceramic interaction at temperatures from 293°C and below were measured by two independent methods, thermovolumetrically, by changes in hydrogen pressure in a Sieverts apparatus and thermogravimetrically, by changes in mass. Volume measurements revealed a dropping of the hydrogen pressure beginning at 200°C and attributable to absorption of hydrogen. Weight measurements revealed first, a small loss of mass attributable to reduction of oxygen and then, a gain of mass owing to absorption of hydrogen. Examination of specimens by the x-ray diffraction method revealed a consistent increase of the lattice c-parameter along the tetragonal axis with increasing hydrogen content in $H_xLa_{1.8}Sr_{0.2}$ ceramic, specimens with up to x = 0.866 hydrogen content having been obtained by impregnation. The superconducting transition temperature was determined on the basis of magnetic susceptibility measurements at a radio frequency and specimens with a hydrogen content corresponding to x = 0.1 or more, did not become superconductors at all. The hydrogen concentration was, in these cases, approaching the Sr concentration and, therefore, the cause of superconductivity suppression could likely be neutralization of holes by hydrogen localized in (1/2,1/2,0) and (0,0,1/2) positions in Cu-O planes. This model, with holes regarded as broken links, is validated by nuclear magnetic-resonance measurements made in an SXP-100 pulsed NMR spectrometer at 60 MHz on a specimen with x = 0.866 and thus, a high hydrogen content. The proton-resonance signal was picked up as a single symmetric line of Gaussian form and 63 kHz wide at any temperature, this width being roughly comparable with the 30 kHz theoretical width based on dipole interaction of a proton with nearest La and Cu nuclei and other protons while hydrogen occupies those positions in a Cu-O plane. The authors thank G.B. Teytelbaum and participants of the seminar held in the Metal Physics Laboratory of the Institute for helpful discussions. Figures 3; tables 1; references 6.

Possible Mechanism of High Energy Release During Burst of Globular Lightning

907J0037C Leningrad ZHURNAL TEKHNICHESKOY FIZIKI in Russian Vol 60 No 3, Mar 90]

[Article by A.S. Tarnovskiy, Kuybyshev State Pedagogical Institute]

[Abstract] Energy release during a burst of globular lightning is reexamined, considering that the various earlier proposed theories do not explain the very high amount of released energy which can reach the 1000 kJ level. The author now proposes that the released energy had been stored not in the globular lightning but in the surrounding space and that the source of additional energy could be an avalanche-like impact condensation of supersaturated atmospheric water vapor. Inasmuch as supersaturation under any given condition is limited, a saturation factor of 10 at 20°C is assumed for a quantitative analysis of the processes according to this mechanism. A globular lightning breaks down and its small fragments scatter around as the pressure drops sharply and the temperature also drops so that condensation of vapor intensifies. The remote air layers above the depression region in which vapor does not condense will compress the air around that region and thus heat it up. A concentric gas dynamic wave is consequently generated at the periphery of the lightning which then propagates toward the center of the latter. According to this theory, supported by observations, a burst of globular lightning is "quiet" under normal conditions without vapor condensation and a "violent" burst of such lightning is rare. When several bursts occur successively in short intervals of time, then only the first one is powerful. According to this theory, power amplification by condensation of atmospheric water vapor should occur upon any sharp pressure drop within a region with supersaturated air. This has been confirmed by sound that was heard coming from an evacuated electric light bulb breaking down in a room humidified to saturation. An important factor is this mechanism is the condensation time, which can be calculated from the relation $4cu\pi r^2 n_0 = -\delta c/\delta t$ (c- vapor concentration, u- thermal velocity of vapor molecules, n_0- initial charge carrier concentration). Another factor is the radius of the condensation region, which depends on the radius of the globular lightning and on the speed of sound in air as well as on the condensation time.

Self-Adaptation in Chaos. New Method of Diagnostic Testing

907J0049B Leningrad PISMA V ZHURNAL TEKHNICHESKOY FIZIKI in Russian Vol 16 No 3, 12 Mar 90 pp 85-88

[Article by V.S, Anishchenko and D.E. Postnov, Saratov State University imeni N.G. Chernyshevskiy]

[Abstract] A new method of diagnostic testing is proposed for application to evolutionary processes with coupled oscillations in self-randomizing systems, change in the control parameters for such a quasi-hyperbolic system of this kind, for instance, is known to lead to structurization of random attractors called bifurcation in chaos. The method involves calculating the distribution density of differences between the oscillation spectra of partial subsystems as a basis for reliable diagnosis of frequency locking and of fully symmetrized random oscillation modes, independent of the structural intricacy of the amplitude spectra. The method is demonstrated on transition to perfectly random synchronization in a six-dimensional system of two symmetrically coupled random oscillators differing only in their base frequency, but otherwise identical. The process is tracked from an initially weak coupling of the oscillators through a gradually stronger one. The authors thank Yu.L. Klimontovich for interest and helpful discussion. Figures 1; references 5.

UDC 517.58

S. Ramanujan on Hypergeometric and Basic Hypergeometric Series

907J0020A Moscow USPEKHI MATEMATICHESKIKH NAUK in Russian Vol 45 No 1, Jan-Feb 90 pp 33-76

[Article by Richard Askey, translated from English by N.M. Atakishiyev and S.K. Suslov]

[Abstract] The impact of S. Ramanujan (born in the year 1888 in the town Erode near Tajore. India) on mathematical analysis is measured by his contribution to the theory of hypergeometric series and their analytic continuations in the form of hypergeometric functions. Hypergeometric series Σc_n are those where c_{n+1}/c_n is a rational function and those truncated on one side ${}_pF_q = \Sigma[(a_1)_n...(a_p)_n x^n/[(b_1)_n...(b_q)_n!$ n from 0 to ∞ converging only for $|x < 1$ when q = p-1 (for all x when q = or > p). A historical review of the background leading up to Ramanujan's involvement with this subject, which includes solution of hypergeometric differential equations and where necessary analytic continuation of other series, is followed by a systematic coverage of Ramanujan's work and relevant biographical data. His contributions include, evaluation of the Euler constant, many continued fractions, most important of which is expansion of the (P- Q)/(P+ Q) fraction on the basis of Dougall's and trinomial recurrence relations for completely balanced ${}_7F_6$ series, validation of Pfaff's sum of ${}_3F_2$ series, reduction of ${}_6F_5$ series to ${}_3F_2$ series, evaluation of series such as ${}_4F_3$ series as a product of $1/\pi$ by rational number or a real irrational square root, asymptotic values of definite series. A special subject are basic hypergeometric series Σc_n where the ratio c_{n+1}/c_n is a rational function q^n of some fixed parameter q. Ramanujan's work in this area covers three periods, 21 identity relations summarizing his contribution in the first period followed by 13 similar ones in the second period. His treatment of theta functions, in the third period, starts with Gauss' triple product and follows it up with a modular transformation leading up to the two Rogers-Ramanujan identities. The author of this treatise on S. Ramnujan thanks P.K. Srinivasan and the trustees of Madras Harbor for assistance in compiling Ramanujan's notes, letters, and publications. References 165.

UDC 517.9

Example of Reaction System With Diffusion Leading to Explosion

907J0053A Moscow DOKLADY AKADEMII NAUK SSSR in Russian Vol 310 No 6, Feb 90 pp 1308-1309

[Article by V.V. Churbanov, Moscow State Technical University imeni N.E. Bauman]

[Abstract] A solution to the Cauchy problem for the system of parabolic equations describing a reaction process with diffusion $u_t - \Delta u = f(u,v)$ and $u_t - \Delta v = g(u,v)$ with continuous initial conditions and any constraints are found in the half-space $(0,+\infty)xR^n$, if the system of ordinary differential equations $du/dt = f(u,v)$ and $dv/dt = g(u,v)$ describing a diffusionless process has a solution at all times $t > 0$ for any initial condition. While the diffusionless system has a steady state, stable in the Lyapunov sense, the steady state of the parabolic system with diffusion becomes unstable in the Neumann problem with zero flux at the boundary, which indicates that diffusion significantly alters the process. An example is shown in which diffusion terms lead to explosion rather than stabilization of the process, inasmuch as the solution to the corresponding Cauchy problem for certain initial conditions approach infinity within a finite time within a bounded region. Such an example is the system $u_t - u_{xx} = f(u,v)$ and $v_t - v_{xx} = 0$, where $v(t,x) = 1/(t+1)^{-1/2}e^{-x^2}/4(t+1)$ satisfies the second equation. Article was presented by Academician V.S. Vladimirov. References 3.

Asymptotic Problems in Theories of Probability and Random Media

907J0017A Moscow TEORIYA VEROYATNOSTEY I YEYE PRIMENENIYA in Russian Vol 35 No 1, Jan-Mar 90 pp 27-34

[Article by A.D. Ventsel, S.A. Molchanov, and V.N. Tutubalin]

[Abstract] Large deviation theorems pertaining to asymptoticity of large numbers or infinitesimally small probabilities are applied to two basic kinds of asymptotic behavior of large deviations: those involved when Cramer's condition of finite exponential moments is to be satisfied and when a "tail" of a power series remains behind a large term approximately equal to the sum of all terms. Three kinds of asymptotic problems involving large deviations in random media are considered: the first involves products of random matrices in the Ferstenberg-Tutubalin theory based on existence of a sequence of non-random numbers, Lyapunov exponents, $\lambda_\nu < \lambda_{\nu-1} < \ldots \lambda_1$ such that their sum is zero and of random subspaces $L_{\nu+1}$ in L_ν in $L_{\nu-1}$ ... in L_1 in R^ν contained successively one by the next in an R^ν space with dim $L_k = \nu - k + 1$ such that $\lim(1/n)\log\|xA_1 \ldots A_n\| = \lambda_k$ as number n becomes infinitely large. Applications of this theory include exponential decrease of energy in a light pulse passing through an optical waveguide with random stationary defects along the path, punctiform spectrum of $-y'' + q(t,\theta)y = Ey$ operators on "Markov" potentials, and behavior of the magnetic field as the time of Hubble flow becomes infinitely long. Two different kinds of such problems are a Gaussian or other weak diffusion process to which the central limit theorem applies and processes with frequent small jumps. For diffusion processes, periodic in time, with averaging in space are available stationary models in which the potential V(x.) does not change in time and nonstationary models in which it does, the time correlations in the latter kind weaken at a faster rate. As an example, consider the Cauchy problem for the parabolic equation $\delta c(t,x)/\delta t = \kappa \Delta c(t,x) + V.c(t,x)$, where $c = c_0 > 0$ at time $t = 0$. Two theorems are stated for stationary models, one establishing an equality for $(1/t)\log[c(t,x)]$ which holds true with certainty as time $t \to \infty$ and one for $(1/t)\log c^p(t,x)$ which holds true for any natural p larger than zero. Two theorems are stated for nonstationary models in which potential V(x,t) has the form of a white noise. The first one pertains to function $\gamma_p(\kappa) = \lim c^p(t,x)$ as $t \to \infty$ representing the regular component ($\kappa > 0$ - viscosity or diffusivity), namely that $\gamma_p(\kappa)/p$ decreases monotonically. The second one pertains to function $\gamma^{\text{tilde}} = \lim(1/t)\log[c(t,x)]$ as $t \to \infty$ representing the fluctuation component, namely that it increases monotonically from -1/2 to 0 as κ increases from 0 to ∞. References 8.

Probability Analysis of Rounding Errors in Floating-Point Arithmetic

907J0017B Moscow TEORIYA VEROYATNOSTEY I YEYE PRIMENENIYA in Russian Vol 35 No 1, Jan-Mar 90 pp 63-71

[Article by N.N. Lyashenko and M.S. Nikulin]

[Abstract] Representation of real numbers and arithmetic operations in the binary system with a floating point are examined from the accuracy standpoint, accuracy being constrained by speed requirement and available memory volume. A limitation on the order that it contain not more than r bits does not significantly limit the accuracy, since overflow of this field will stop the computation, but limitation that the mantissa contain not more than d bits will limit the accuracy. Only the round-off operator fl_d is given further consideration, therefore, following a statement of three axioms which define a round-off operator fl, in addition to the first axiom, that its domain is the set R^1 of all real numbers. Seven properties of the round-off operator fl_d are stated in the form of an already proven lemma, one of these properties being that the operations direct sum and direct product are commutative, but neither associative nor distributive. There follows a theorem pertaining to operations on two independent uniformly distributed random quantities X and Y which establishes lower and upper bounds for the difference of distribution functions $F_{d.q.(X,Y)}(x) - F_{X/Y}(x)$ and for the difference of distribution functions $F_{d.p.(X,Y)}(x) - F_{XxY}(x)$ (d.q.- direct quotient ?, d.p.- direct product). Three kinds of rounding error are defined next: absolute error ε_a, relative error $\varepsilon_r = (1/x)fl_d(x)-1$ for nonzero x, and absolute mantissa error $\varepsilon_m = \text{mant}(fl_d(x)-\text{mant}(x)$. Three lemmas are stated which yield the probability distribution, the absolute error of a uniformly distributed quantity and the moments of that distribution, the absolute error of such a quantity being a random quantity with a symmetric bounded probability distribution to which the local limit theorem applies. Two theorems are proved pertaining to the density of the absolute rounding error, a piecewise-continuous function, of a random quantity with an arbitrary probability density. Another theorem is proved pertaining to a sequential algorithm of d-bit multiplication with a floating point which yields a sequence of values mutually independent and uniformly distributed on the half-open interval [1,2). For a Markov sequence z_j generated by such an algorithm, there exists, according to this theorem, a limiting distribution of states of the mantissa z_j Markov chain. Application of this theorem is demonstrated on an experiment, the authors having developed a program which includes multiplication with fast rounding procedures in the integer representation t = [mant(z)- 1], a procedure for computing the probability matrix of transitions, and a procedure for computation of the limiting distribution proper. For d = 5 the vector of final probabilities yields a limiting distribution with p_{min} = 3.226328E-02 and p_{max} = 8.425150E-02, thus quite different than a uniform one. References 8.

22161
21

NTIS
ATTN: PROCESS 103
5285 PORT ROYAL RD
SPRINGFIELD, VA 22161

Foreign Broadcast Information Service (FBIS) and Joint Publications Research Service (JPRS) publications contain political, military, economic, environmental, and sociological news, commentary, and other information, as well as scientific and technical data and reports. All information has been obtained from foreign radio and television broadcasts, news agency transmissions, newspapers, books, and periodicals. Items generally are processed from the first or best available sources. It should not be inferred that they have been disseminated only in the medium, in the language, or to the area indicated. Items from foreign language sources are translated; those from English-language sources are transcribed. Except for excluding certain diacritics, FBIS renders personal and place-names in accordance with the romanization systems approved for U.S. Government publications by the U.S. Board of Geographic Names.

Headlines, editorial reports, and material enclosed in brackets [ ] are supplied by FBIS/JPRS. Processing indicators such as [Text] or [Excerpts] in the first line of each item indicate how the information was processed from the original. Unfamiliar names rendered phonetically are enclosed in parentheses. Words or names preceded by a question mark and enclosed in parentheses were not clear from the original source but have been supplied as appropriate to the context. Other unattributed parenthetical notes within the body of an item originate with the source. Times within items are as given by the source. Passages in boldface or italics are as published.

SUBSCRIPTION/PROCUREMENT INFORMATION

The FBIS DAILY REPORT contains current news and information and is published Monday through Friday in eight volumes: China, East Europe, Soviet Union, East Asia, Near East & South Asia, Sub-Saharan Africa, Latin America, and West Europe. Supplements to the DAILY REPORTs may also be available periodically and will be distributed to regular DAILY REPORT subscribers. JPRS publications, which include approximately 50 regional, worldwide, and topical reports, generally contain less time-sensitive information and are published periodically.

Current DAILY REPORTs and JPRS publications are listed in *Government Reports Announcements* issued semimonthly by the National Technical Information Service (NTIS), 5285 Port Royal Road, Springfield, Virginia 22161 and the *Monthly Catalog of U.S. Government Publications* issued by the Superintendent of Documents, U.S. Government Printing Office, Washington, D.C. 20402.

The public may subscribe to either hardcover or microfiche versions of the DAILY REPORTs and JPRS publications through NTIS at the above address or by calling (703) 487-4630. Subscription rates will be provided by NTIS upon request. Subscriptions are available outside the United States from NTIS or appointed foreign dealers. New subscribers should expect a 30-day delay in receipt of the first issue.

U.S. Government offices may obtain subscriptions to the DAILY REPORTs or JPRS publications (hardcover or microfiche) at no charge through their sponsoring organizations. For additional information or assistance, call FBIS, (202) 338-6735,or write to P.O. Box 2604, Washington, D.C. 20013. Department of Defense consumers are required to submit requests through appropriate command validation channels to DIA, RTS-2C, Washington, D.C. 20301. (Telephone: (202) 373-3771, Autovon: 243-3771.)

Back issues or single copies of the DAILY REPORTs and JPRS publications are not available. Both the DAILY REPORTs and the JPRS publications are on file for public reference at the Library of Congress and at many Federal Depository Libraries. Reference copies may also be seen at many public and university libraries throughout the United States.